Available online at www.CivileJournal.org

Civil Engineering Journal

(E-ISSN: 2476-3055; ISSN: 2676-6957)

Vol. 12, No. 01, January, 2026

Assessment of Red Sea Shoreline Dynamics Through Satellite Imagery and GIS Analysis

Khaled Mahmoud Abdel Aziz [1*]

[1] *Department of Civil Engineering, College of Engineering in Al-Kharj, Prince Sattam bin Abdulaziz University, Al-Kharj 11942, Saudi Arabia.*

Received 03 November 2025; Revised 19 December 2025; Accepted 27 December 2025; Published 01 January 2026

Abstract

Monitoring and analyzing coastal dynamics is essential due to continuous shoreline changes driven by natural processes and human activities with significant environmental and economic impacts. This study aims to quantitatively assess shoreline change along the Red Sea coast using integrated remote sensing and Geographic Information Systems (GIS) techniques. Multi-temporal satellite imagery from 1980 to 2025 was processed to extract shoreline positions, and shoreline change rates were calculated using the EPR method to determine patterns of erosion and accretion. The study area extends along the northwestern part of Saudi Arabia within the Tabuk region, covering Wadi al Ayn, NEOM Port, and the villages of Al Muwaylih, As Sawrah, Sharma, Al Khuraybah, and Qiyal. The results reveal that erosion rates exceed accretion rates across most shoreline segments during the study period. The average EPR of accretion reached 1.13 m/yr, while erosion recorded a higher magnitude with an average rate of −1.99 m/yr. Spatial analysis showed a total accretion area of 1.634 km² compared to a substantially larger erosion area of 19.624 km². This study lies in providing a comprehensive, long-term spatiotemporal assessment of shoreline dynamics using consistent satellite-based measurements, contributing updated baseline data for coastal management and sustainable development planning in the Red Sea region.

Keywords: Shoreline; DSAS; Remote Sensing; GIS; ENVI 5.3; ArcGIS 10.8; EPR; LRR; NSM; SCE; SDG; Accretion and Erosion.

1. Introduction

Nearly half of the world's population resides near seas and oceans, making the evaluation and mapping of shoreline dynamics a key component of sustainable development and urban planning. Although coastal zones represent less than 20% of the global land surface, they support dense populations and extensive economic activities. Globally, more than 1.6 million km of coastline exist, and approximately 84% of countries possess some form of shoreline, including marine or inland coastal waters [1]. Shoreline change refers to the alteration of the land–water boundary caused by natural processes such as erosion, sediment deposition, and sea-level rise, as well as anthropogenic influences including coastal development and climate change [2]. Erosion rates vary spatially due to local factors including vegetation cover, offshore bathymetry, bluff stratigraphy, drainage patterns, groundwater conditions, and land-use management strategies. Human activities such as beach sand mining, offshore dredging, dam construction, and shoreline infrastructure development further intensify these processes. Multi-temporal analysis that encompasses long observation periods and extreme events is therefore essential for accurate shoreline assessments. Globally, coastal erosion has been recognized as a serious environmental and socio-economic concern, and shoreline change analysis is widely applied to identify vulnerable areas and define coastal hazard indices [3]. Due to the development of massive coastal megaprojects in the early 2000s, coastal urbanization in the Arabian Gulf region has increased since the oil boom of the 1970s. Increased environmental

* Corresponding author: km.mahmoud@psau.edu.sa

https://doi.org/10.28991/CEJ-2026-012-01-09

pressures, changes in land use and cover, and altered habitats are all consequences of this expansion. Because they offer affordable, non-intrusive mapping options for coastal areas, remote sensing technologies have become essential for tracking these changes. However, RS applications are still spatially dispersed throughout the region, often concentrating on specific metropolitan areas rather than long-term regional change patterns or larger coastal systems [4]. Reliable spatial datasets and established geospatial approaches are critical to tracking the 17 Sustainable Development Goals on a global scale. Geospatial technologies have been suggested as methods to enhance SDG-based monitoring, visualize regional disparities, and improve goals 5, 8, 10, and 17. In Saudi Arabia, it has been acknowledged that integrating GIS, big-data analytics, and satellite-derived data is crucial to accomplishing Vision 2030 goals and bolstering national SDG monitoring frameworks [5].

The detection and interpretation of shoreline migration have been further enhanced by developments in satellite resolution and temporal coverage, supporting applications in environmental monitoring, urban planning, catastrophe risk assessment, and climate research. The importance of GIS and remote sensing in impact assessment and mitigation planning has been brought to light by the strong correlation between climate change drivers, such as sea-level rise and increased storm activity, and coastline erosion or accretion [1]. To assist thorough coastal zone evaluations, GIS platforms incorporate a variety of datasets, including time-series coastline positions, topographic data, and socioeconomic variables [6].

Shallow tidal flats, wadi distributary channels, sabkhas, sharms, khors, lagoons, and dynamic oceanographic processes are just a few of the intricate geomorphological characteristics that have created the Red Sea's coastline morphology. The hydrological connection between the Red Sea and the Indian Ocean through the Strait of Bab al-Mandab produces a distinct water exchange system that contributes to the renewal of coastal waters and influences sediment transport patterns. Strong wave activity, longshore sediment drift, and sporadic storm occurrences all contribute to shoreline changes and regulate the rates of accretion and erosion along the coast. The northern sector is affected by winter northwesterly winds connected to Mediterranean storm systems, while the southern shoreline is affected by southeasterly winds connected to the Arabian Sea monsoon. Seasonal wind regimes also have a significant impact. There is a gap in thorough shoreline-change modeling throughout the Red Sea region due to the lack of quantitative integration of hydrodynamic processes, wind systems, and sediment transport at consistent spatial and temporal scales, despite the recognition of these driving mechanisms. This underscores the need for long-term, geospatially standardized assessments [7].

Alharbi (2020) [8] analyzed shoreline changes along the Rabigh coast from 1986 to 2019 using multi-temporal remote sensing data integrated with GIS and the Digital Shoreline Analysis System (DSAS). Shoreline change rates were calculated using the EPR and LRR methods across three periods (1986–1998, 1998–2005, and 2005–2019), coinciding with rapid industrial and urban development in the region, including the establishment of major facilities such as desalination and power plants, cement and petroleum industries, residential expansion, and large-scale economic projects, most notably King Abdullah Port and King Abdullah Economic City (KAEC). The results indicated that coastal erosion dominated the study area, as 82.61% of shoreline transects exhibited erosion based on LRR analysis. The highest accretion rate was recorded near King Abdullah Port at approximately 18.78 ± 0.48 m/year, while the maximum erosion rate reached −23.22 ± 0.48 m/year. Furthermore, EPR results for the 2005–2019 period showed that erosion intensified in several locations, exceeding −47.21 ± 1.41 m/year, particularly along the coastlines of King Abdullah Port, KAEC, Sharm Rabigh, and Ra’s Arab. In contrast, localized shoreline accretion was observed in certain areas, which was associated with beach stabilization efforts and increased tourism, recreational activities, and economic development, highlighting the strong influence of human activities on shoreline dynamics along the Rabigh coast.

Alharbi et al. (2023) [7] identified human activities, infrastructure development, and the establishment of industrial zones such as King Abdullah Port, KAEC Beach, and Sharm Rabigh as the main drivers of changes along the Rabigh shoreline. Future developments and activities affecting the maritime environment and wadi outfalls may further increase the shoreline's vulnerability. The study aimed to forecast the spatial positions of the Ash Shu’aybah and Al Mujayrimah coastlines along the eastern Red Sea of Saudi Arabia for the period 2022–2042 and to quantify shoreline change rates. Sentinel-2 and Landsat satellite imagery were employed, and results from both datasets were comparatively analyzed. The Digital Shoreline Analysis System (DSAS v5.0) integrated with ArcGIS 10.8 was used to process the satellite data, while shoreline change rates were assessed using the Shoreline Change Envelope (SCE), Net Shoreline Movement (NSM), End Point Rate (EPR), and Linear Regression Rate (LRR) models. Findings revealed that erosion is the dominant process driving coastal degradation, accounting for approximately 75.41% and 89.07% of the observed changes in the Sentinel-2 and Landsat analyses, respectively. Mean erosion rates were estimated at −3.25 m/yr and −2.12 m/yr for Sentinel-2 and Landsat datasets, with the central portion of the coastline, particularly Segment 2, experiencing the most severe erosion.

Al-Zubieri et al. (2018) [9] investigated the morphological evolution of the Jazan coastline, one of the fastest-growing urban centers along the southern Red Sea coast of Saudi Arabia, over a 30-year period (1987–2017). Using Geographic Information Systems (GIS) and multi-temporal remote sensing data from TM and ETM satellite images,

together with an urban growth map digitized from Google Earth Pro, the study assessed spatial patterns of shoreline change and urban expansion. Photo-interpretation techniques were applied to quantify land reclamation, erosion, and deposition processes. The results revealed substantial geomorphological and anthropogenic changes, characterized by rapid residential expansion and a noticeable seaward advancement of the shoreline. Landfilling activities were most concentrated in the northern and central coastal sectors between 2000 and 2013, while localized erosion and accretion dominated during the earlier period (1987–2000). The relative intensity of change reached 14.33% between 1987–2000, increased sharply to 58.56% during 2000–2013, and declined to 27.11% from 2013–2017. Residential areas expanded significantly from 23.31 km² in 1987 to 25.32 km² in 2000, 63.37 km² in 2013, and 67.90 km² in 2017, mainly driven by large-scale anthropogenic interventions, particularly the development of the northern Economic City between 2003 and 2013.

Al-Zubieri et al. (2020) [10] investigated shoreline changes along the coastline between Al Lith and Ras Mahasin, Saudi Arabia, for the period 1984–2018 using Geographic Information Systems (GIS) and automated analysis through the Digital Shoreline Analysis System (DSAS). Multi-temporal satellite imagery was employed to extract seven shoreline positions for the years 1984, 1986, 1990, 1994, 1998, 2014, and 2018 using the TCT method. The results showed that the study area experienced persistent and widespread erosion throughout the 34-year period, with the highest erosion rates concentrated in the southern sectors adjacent to sea headlands, while only limited accretion was observed in small portions of the northern area. The shoreline instability was mainly attributed to natural factors, including intense wave activity, storm impacts, and sediment transport induced by longshore currents. Using the EPR model, future shoreline positions were predicted for 2022 and 2038, indicating continued landward retreat of the coastline despite the uncertainties associated with modeling accuracy. The LRR method classified shoreline evolution into five categories ranging from very high erosion (−11.84 to −7.85 m/yr) to high accretion (1.28 to 14.44 m/yr). Overall, the findings demonstrated strong spatial variability in shoreline dynamics and confirmed that large sections of the coast between Al Lith and Ras Mahasin are highly vulnerable to accelerated coastal degradation.

Niang (2020) [11] analyzed shoreline changes along the Yanbu coastal sites from 1965 to 2019 using six multisource and diachronic remote sensing datasets processed with GIS techniques. Change rates were computed through the Digital Shoreline Analysis System (DSAS), employing the EPR function for successive period pairings (1965–1980, 1980–1988, 1988–2000, 2000–2010, 2010–2019) and the LRR and Weighted Linear Regression (WLR) functions for the overall 54 year period. The study period was marked by progressive human colonization, urbanization, and economic development, including Yanbu's designation as the kingdom's industrial gateway. Results indicate that accretion dominates, particularly within the industrial city, where the highest rates and maximum accretional values were observed. This trend is largely attributed to coastal industrial development, including the construction and expansion of the King Fahd Industrial Port and the Commercial Port, which involved extensive backfilling and destruction of islands and reefs. LRR analysis revealed that approximately 54.92% of transects exhibited accretion trends, with a maximum accretion rate of 32.32 ± 2.27 m/yr, while the maximum erosion rate along some transects reached −32.7 ± 2.27 m/yr. EPR analysis showed that shoreline advancement rates ranged from 68 to 190 m/yr, whereas maximum erosion varied from −10.9 to −203 m/yr. Spatial patterns varied along successive coastlines, with accretion concentrated in Sharm Yanbu, the commercial harbor, and the industrial city, and erosion more pronounced in certain segments of Sharm Yanbu and the industrial area. Overall, the study demonstrates that human activities are the primary drivers of shoreline change in Yanbu over the past five decades.

Daoudi & Niang (2021) [12] monitored the spatiotemporal evolution of Jeddah's shoreline and assessed its impacts on coastal geomorphology using the Digital Shoreline Analysis System (DSAS) over the period 1951–2018. The study applied the LRR method to identify long-term shoreline displacement trends and the EPR method to quantify changes between successive time intervals. The results revealed that shoreline accretion dominated the coastal dynamics, particularly along the port area, where seaward advancement reached a maximum rate of 47.6 ± 0.2 m/year with an average rate of 17.8 m/year. These relatively high rates were mainly attributed to ongoing land reclamation projects and the continuous expansion of port infrastructure. Approximately 23 km² of sea and islets were reclaimed for port infrastructure development, resulting in significant morphodynamic modifications to several geomorphological units and altering the natural littoral system. Shoreline change analysis over successive periods revealed considerable temporal variability. Between 1951 and 1966, the average shoreline displacement rate was 5.72 m/year, with a minimum erosion rate of −7 m/year and a maximum accretion rate of 44 ± 0.52 m/year. During 1972–1986, erosion decreased to −3.4 ± 0.87 m/year, while accretion peaked at 180.8 ± 0.87 m/year. The period 1986–2003 exhibited the lowest accretion activity, with a maximum rate of only 33.39 ± 0.67 m/year. Between 2003 and 2010, the average shoreline change was 0.8 ± 0.46 m/year, with minimal erosion (−0.05 ± 0.46 m/year) and an increase in accretion to 107.5 ± 0.46 m/year. The most recent interval, 2010–2018, associated with port expansion toward the sea, recorded the highest accretion rate of 210.93 ± 1.46 m/year, while erosion remained limited at −1.69 ± 1.46 m/year, and the average rate of shoreline change was 2.27 ± 1.46 m/year.

Alharbi & Niang (2025) [13] used multi-temporal Landsat images in conjunction with GIS and the Digital Shoreline Analysis System (DSAS) to examine the geographical and temporal changes of the Al Qunfudhah shoreline between

1984 and 2020. Automated methods, most notably the Canny edge identification algorithm, were used to derive shoreline positions. The EPR and LRR methods were used to compute shoreline change rates. The shoreline showed an overall tendency of minor advancement over the 36-year period. In the northern sector, where a corniche road was constructed, the average accretion rates were 3.63 m/year (LRR) and 4.17 m/year (EPR), while the maximum rates were 12.43 m/year (LRR) and 13.36 m/year (EPR), especially in the northern portion, where a corniche road was constructed. On the other hand, the most notable erosion happened close to the boat port, with average rates of −1.23 m/year (LRR) and −1.08 m/year (EPR) and maximum rates of −24.4 m/year (LRR) and −20.9 m/year (EPR). These results provide a scientific foundation for sustainable coastal management along the Al Qunfudhah coastline and emphasize the regional heterogeneity of shoreline dynamics.

Colak (2024) [14] used GIS, remote sensing, and the Digital Shoreline Analysis System (DSAS) to perform a spatiotemporal study of coastal alterations along the Oman coast over a 22-year period (2000–2022). The Canny edge detection technique was used to automatically identify shoreline positions, resulting in accurate and comprehensive representations of the coastline. Rates of accretion and erosion were measured using statistical techniques such as LRR, EPR, and NSM, which captured both long-term and short-term trends. The findings show that accretion is more common along the coast, with erosion occurring in certain places. Natural processes were found to have less of an impact on coastal morphology than human actions, especially the building of artificial structures. The study underlines the significance of ongoing monitoring for sustainable management, tourism, and urban development along the Oman coast, as well as the crucial role that coastline changes play in forming the coastal ecosystem.

Teillet et al. (2025) [15] investigated the morphodynamic evolution of the shoreline and coral reef coverage along the Arabian Sea coast of Oman over the past five decades (1972–2022), focusing on the Bar Al Hikman Peninsula, the largest low-lying coastal area in Oman. By combining sedimentological fieldwork with 50 years of satellite image analysis, the study documents significant coastal changes, including a 60% reduction in the surface area of the main coral reefs. This reef decline has led to rapid shoreline erosion, with half of the southern shoreline retreating northward at rates exceeding 1 m/year, and localized sections (6%) experiencing extreme erosion of over 10 m/year. The ongoing reef degradation is likely to intensify shoreline retreat, accelerate the landward migration of barrier bars, threaten intertidal ecosystems, and cause extensive inland migration of coastal sabkhas, especially with projected sea-level rise by 2050. These findings provide a critical baseline for understanding Oman's Arabian Sea coastline dynamics and emphasize the need for effective coastal management and policy strategies to mitigate environmental risks.

Between 1965 and 2020, Daoudi et al. (2024) [16] examined the environmental effects of coastal alterations along the Jeddah coastline. Like other coastal areas, Jeddah's coastal zones have experienced significant urban and economic development, which has resulted in significant changes at the land–water interface. This development includes the infilling of marshes, shallows, and coral reefs. Aerial photos (1951, 2009), Corona images (1965, 1966, 1972), Landsat (1975, 2013), SPOT (1986, 2010), Sentinel (2018, 2020), historical maps (1884), and field surveys were among the multi-source spatial data used in the study. Vulnerability was evaluated and shoreline change rates were estimated using the Digital Shoreline Analysis System (DSAS). Significant surface changes were found in the results, including erosion in some locations of the seashore and infilling in other others. The study highlights the significance of integrated coastal planning, which combines environmental sustainability with geomorphological analysis. It also shows that other parts of Saudi Arabia may use these methods.

Sarrau et al. (2025) [17] used multi-temporal remote sensing data and a customized algorithm to track the shape and evolution of the UAE shoreline from 1991 to 2021. The findings demonstrated that, as seen in Fujairah and Abu Dhabi, large-scale urban expansion and port development were the main causes of coastline modifications. Prior to 2013, when urbanization was at its fastest, the majority of the coastal evolution took place; after that time, the coastline remained largely steady. Sediment accumulation caused changes in nearshore sandbanks, which led to a progressive seaward extension. However, not all places were accreting, as parts of the western UAE coastline continued to erode. The study suggested using higher-resolution satellite imagery to improve monitoring accuracy in subsequent research and improving shoreline detection algorithms to better differentiate sandbanks from actual coastlines.

Due to their high sensitivity to wind and sea pressures and limited supply of sediment, coasts in arid regions are particularly vulnerable to the effects of climate change. In order to give probabilistic forecasts of shoreline evolution over a 130 km section of the Duba coast in Saudi Arabia, inside the NEOM project region, Alamery et al. (2025) [18] carried out this study. In order to simulate wave dynamics and shoreline evolution, the study coupled integrated numerical models with satellite imagery analysis from 1985 to 2024. The regional models COSMO-CLM and RegCM were used to dynamically downscale climate projections from CMIP6, and a Bayesian framework was used to account for uncertainty at every level of the modeling process and mean Net coastline Movement (NSM) by 2100 ranging from −8.1 m under the low-emission scenario SSP1-2.6 to −25.6 m under the high-emission scenario SSP5-8.5, and 95% confidence intervals reaching −47.9 m, the results clearly show an acceleration in coastline retreat. The anticipated rise in sea level, which might reach 48.3 cm (±15.8 cm), along with an increase in major wave height of up to 40%, with a mean of 1.95 m, are the primary causes of this erosion.

The majority of these studies mainly concentrated on the spatial and statistical description of shoreline advance and retreat rates, with only a partial consideration of human activities and urban expansion, despite the progress made by earlier research in analyzing coastal changes using Geographic Information Systems (GIS), remote sensing techniques, and the Digital Shoreline Analysis System (DSAS). They did not, however, produce precise forecasts of future shoreline evolution under continuous urban growth and climate change, nor did they sufficiently examine the detailed impact of natural processes including wave dynamics, coastal currents, sediment transport, and sea-level rise. Furthermore, these studies did not evaluate the related social and environmental consequences, such as the effects on local economic activity, coastal ecosystems, and coastal vulnerability.

The study area is situated along the northwestern coast of the Kingdom of Saudi Arabia on the Red Sea, extending from Wadi al Ayn in the south, through NEOM Port (formerly Duba), and the villages of Al-Muwaylih, Al Sawrah, Sharma, and Al Khuraybah, to Qiyal village in the far north. This coastal zone falls within the boundaries of the NEOM Project, one of Saudi Arabia's most ambitious strategic development initiatives, designed to stimulate sustainable urban and economic growth. The project includes several major developments such as THE LINE, Oxagon, Trojena, and Sindalah, which aim to transform the region into a modern, innovative coastal hub.

Although this area has gained increasing strategic importance and is undergoing rapid development, most previous studies of shoreline change along the Saudi Red Sea coast have concentrated on locations such as Rabigh, Jazan, Yanbu, and Jeddah. As a result, detailed investigations that utilize multi-temporal satellite imagery and GIS-based shoreline analyses for the NEOM coastal zone remain limited. This shortage of focused research represents a clear knowledge gap regarding the long-term mechanisms governing shoreline evolution and sediment dynamics in the area.

Accordingly, the main objective of this study is to examine and quantify the spatial and temporal variations of the shoreline along the study area from 1980 to 2025. By applying remote sensing techniques integrated with GIS analysis, erosion and accretion rates are calculated to provide a scientific foundation for assessing coastal stability, supporting sustainable shoreline management, and guiding future development planning within the NEOM region.

This article is structured as follows: the study area is presented first, followed by the materials and methods section. The results and discussion are then provided, and finally, the article concludes with conclusions and recommendations.

2. Study Area

The study area is located along the eastern coast of the Red Sea in the Kingdom of Saudi Arabia, extending from Wadi Al-Ayn and passing through NEOM Port (formerly Duba) and the villages of Al Muwaylih, As Sawrah, Sharma, and Al Khuraybah, reaching Qiyal village, as illustrated in Figure 1. This area was selected due to its direct relevance to the strategically significant NEOM project. Launched in 2017, NEOM aims to develop an innovative region powered entirely by renewable energy and guided by modern sustainability principles, as shown in Figure 2 [19].

Figure 1. Shows a detailed view of the study area along the Red Sea coast of the Kingdom of Saudi Arabia, from Wadi al Ayn to the village of Qiyal [20]

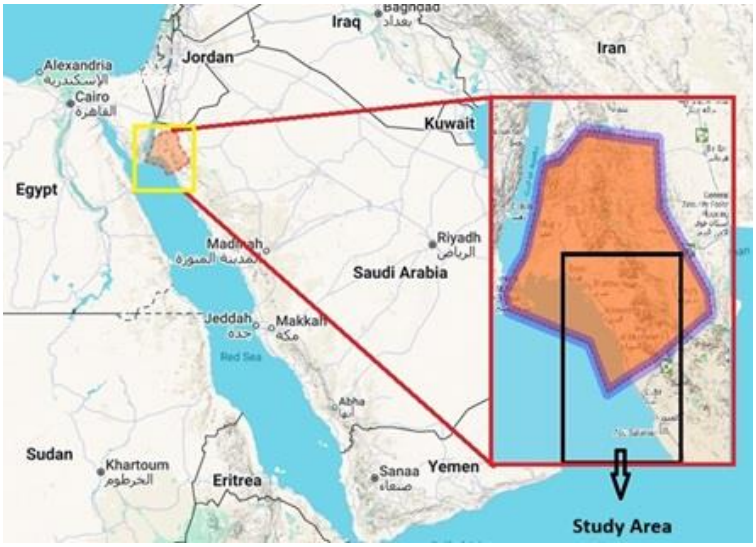

Figure 2. A map depicting the study area, a portion of which is located within the NEOM project in the Kingdom of Saudi Arabia [21]

The study area also includes NEOM Bay Airport, located in central Sharma village in the Tabuk region, which plays a key role in supporting the project's infrastructure [22, 23]. In addition, it encompasses NEOM Port, recognized among the world's advanced ports and considered a major hub for economic activity in the region [24].

3. Materials and Methods

3.1. Data Sources

An essential tool for medium-spatial-resolution earth observations is Landsat images. It is extensively utilized for monitoring the environment globally, including changes in vegetation and coastlines [25]. Coastal dynamics in the study area were examined through the integration of Geographic Information Systems (GIS) and remote sensing methods. The Digital Shoreline Analysis System (DSAS) tool within the GIS framework was utilized to quantify shoreline variations based on geometrically corrected Landsat imagery, while shoreline extraction was performed using ENVI v5.3 software. These images cover the period from 1980 to 2025 across five intervals (1980, 1990, 2000, 2013, and 2025), with spatial resolutions of 30 and 60 meters. The images were obtained from the freely accessible Landsat archive provided by the U.S. Geological Survey [26]. Table 1 presents the details of the satellite images used in this study. Several criteria were considered when selecting the images, including image quality and the avoidance of satellite scenes affected by cloud cover that could impact the study area.

Table 1. Specifications of the Satellite Imagery Employed in the Study

Spacecraft ID	Sensor ID	Date Acquired	Spatial Resolution
LANDSAT_2	MSS	1980-10-23	60 m
LANDSAT_5	TM	1990-03-24	30 m
LANDSAT_7	ETM	2000-03-27	30 m
LANDSAT_8	OLI_TIRS	2013-05-26	30 m
LANDSAT_8	OLI_TIRS	2025-08-23	30 m

3.2. Methodology

This study employed multispectral Landsat satellite imagery spanning the period from 1980 to 2025 to analyze shoreline dynamics. The primary software packages used for data processing and analysis included ArcGIS 10.8, ENVI 5.3, and (DSAS). These tools were utilized to quantify shoreline change rates and patterns. The assessment involved the computation of four key statistical indicators: (SCE), (NSM), (EPR), and (LRR), were calculated from the following methodological steps outlined in the subsequent section.

A- Data Acquisition

- Landsat satellite images representing different periods within the study area (1980–2025) were obtained from [26], see Table 1.

B- Coordinate Reference System

- All satellite images were projected to the Universal Transverse Mercator (UTM) coordinate system, Zone 36 N.

C- Image Preprocessing

- Radiometric calibration was applied to all images.
- FLAASH atmospheric correction was performed using ENVI 5.3 software to improve radiometric accuracy.

D- Shoreline Extraction

- Shorelines for the five Landsat images were delineated by separating seawater from land areas using the color slice technique in ENVI 5.3.
- The extracted shorelines were exported as shape files for analysis in ArcGIS 10.8.

E- Data Preparation

- In ArcGIS 10.8, the shoreline polygons obtained from ENVI 5.3 were converted into polyline features suitable for DSAS analysis.
- The DSAS v5 tool was downloaded from [27].
- A personal geodatabase was created, containing feature classes for both coastlines and baseline.

F- Baseline and Transect Generation

- A baseline was established approximately 3,500 m landward from the oldest shoreline (1980).
- Using DSAS, transects were generated perpendicular to the baseline at 50 m intervals.

J- Shoreline Change Analysis

The shoreline and baseline data were statistically analyzed using the DSAS program. For every period, the following shoreline change metrics were computed: EPR, NSM, and SCE. Finally, the LRR for the years 1980–2025 was calculated [28]. A flowchart outlining the processes of the study's methodological workflow has been created in order to further describe the methodology, as seen in Figure 3.

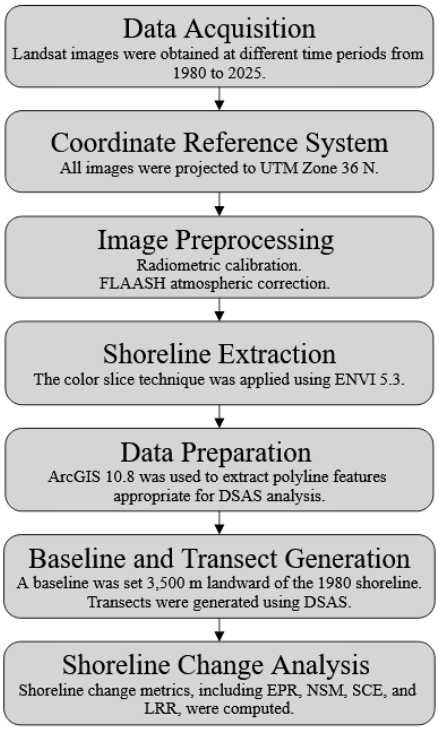

Figure 3. Diagram summarizing the shoreline change analysis methodology

3.3. Digital Shoreline Analysis System (DSAS)

Users can calculate shoreline rate-of-change data from multiple historical locations using the Digital Shoreline Analysis System (DSAS), an extension within Esri ArcGIS Desktop. It offers an automated way to set up measurement sites, compute rates, and give the statistical information required to evaluate rate robustness. Studies have shown that employing DSAS enables both the computation of average erosion and accretion rates for a study area and clear shoreline analysis [29]. For the purpose of implementing efficient coastal zone management, DSAS offers useful information [30].

The U.S. Geological Survey's Coastal Change Hazards project utilizes DSAS to provide a consistent and reproducible set of regression rates, applicable to large datasets collected at varying scales. DSAS is versatile and can be used in any application that tracks positional changes over time, including monitoring riverbank shifts, glacier boundaries in historical aerial imagery, or alterations in land use and land cover [31].

In addition to providing rate-of-change statistics and arithmetical information necessary to guarantee the consistency of the calculated conclusions, the software is designed to assist in the computation of shoreline change [32]. Using a variety of models or techniques, including linear regression rate, endpoint rate, average of rates, and others, it computes rates of change, establishes a baseline, and generates orthogonal transactions that show separation along the coast [33]. The most fundamental use of DSAS involves utilizing multiple layers to represent a specific shoreline feature such as the mean high water mark or cliff edge at a given point in time. DSAS includes several statistical change metrics, including SCE, EPR, NSM, LRR and WLR, all of which analyze shoreline positions over time. By deriving historical rates of change, DSAS can also be used to predict future shoreline behavior, assuming that the physical, natural, or human induced processes driving past changes continue in a similar manner [34]. In general, DSAS can be used to map the historical locations of coastlines during the time period covered by currently available spatial data (such as maps and aerial photos); the historical trends and variations of particular or chosen transects are assessed (discrete alongshore positions). As long as the physical, natural, or human-caused forcing responsible for the historical change displayed at the site remains constant, the DSAS output can be used to estimate shoreline change at specific transects, study shoreline geometry, including foreshore steepening, and predict patterns of shoreline behavior using historical rate of change trends as an indicator of future trends [35].

Since the NSM statistic is based on the separation between the oldest and youngest shorelines, the units are in meters. The NSM was calculated using Equation 1.

$$NSM = d_i - d_o \quad (1)$$

In this case, d_0 is the oldest dated shoreline distance (m), while d_i is the youngest shoreline distance (m). When the NSM value is positive, the shoreline exhibits seaward silting and an advancing shoreline. On the other hand, the shoreline erodes and retreats toward the land when the NSM value is negative [36]. It was also discovered that NSM values produced data that might be used in future forecasting research [37].

EPR determined by dividing the distance separating the earliest and latest shoreline positions by the elapsed time period. The formula used for its calculation is as follows:

$$EPR = (D_{new} - D_{old)} / (T_{new} - T_{old}) \quad (2)$$

where, T_{new} is the most recent shoreline's year, T_{old} is the oldest shoreline's year, D_{new} is the most recent shoreline's distance, and D_{old} is the oldest shoreline's distance [38].

The main benefits of the EPR are its simple computation and the fact that it only requires two shoreline data points. The main drawback is that the data on shoreline behavior offered by more than two shorelines is ignored when there are more than two available [37]. Despite this drawback, EPR is strongly supported in studies. It is mostly used to detect accretion and erosion throughout time [29].

Rather than a pace, the SCE gives a distance. The SCE value indicates the greatest separation between all shorelines that cross a particular transect, see Figure 4. The SCE value is constantly positive because there is no sign indicating the complete distance between two shorelines. A few changes in the coastline during the research period are shown by values close to zero, which are caused by the SCE index's features. When examining sites that haven't changed over time, this tool is quite helpful [37].

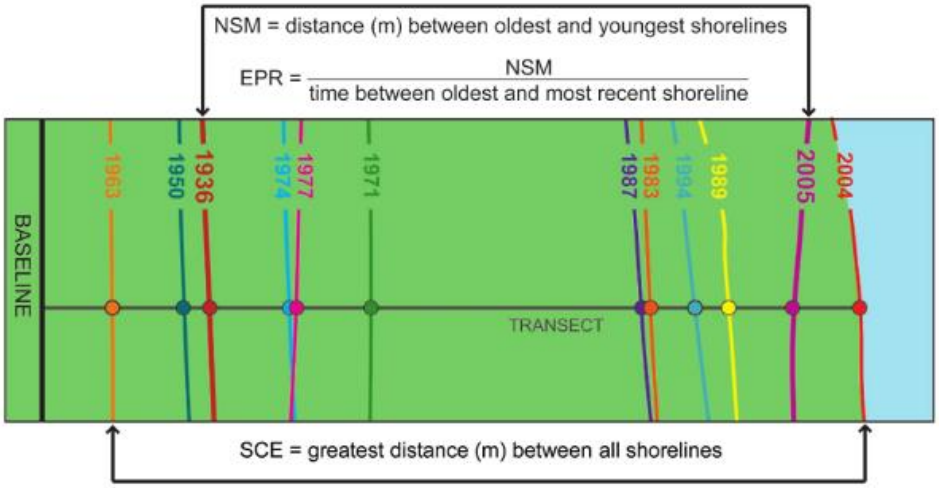

Figure 4. Illustration of NSM, SCE, and EPR [39]

A least-squares regression line based on all shoreline positions along each transect is used to calculate the LRR in meters per year. This method works well for determining long-term coastal change rates and assessing shoreline evolution trends. Unlike the EPR method, the LRR technique can incorporate multiple shoreline positions, thus addressing the limitations associated with EPR [40].

4. Results and Discussion

Using ENVI software, the shoreline of the study area was delineated from five Landsat images, allowing for the separation of land from water in each image. Additionally, shoreline change rates for the different time periods were calculated using ArcGIS software and the DSAS tool. The following paragraphs present the findings of these analyses.

In Figure 5, which illustrates the NSM values representing shoreline changes from 1980 to 1990, a clear gradient and significant variation in shoreline erosion can be observed. The erosion extends from transect 2273 at the shoreline of Wadi Sarr in Al Muwaylih village, passing through the shorelines of As Sawrah, Sharma, and Al Khuraybah villages, up to the shoreline of Qiyal village at transect 3925, where the maximum erosion reached approximately -1229 m. This area is considered part of the NEOM project. A few areas within the same region also show limited accretion, ranging between 45 m and 377 m. Additional erosion was observed starting from transect 1097 at the shoreline opposite Jabal Shar near NEOM Port (formerly Duba Port) and extending to the first transect opposite Wadi al Ayn shoreline, where the maximum erosion was around -248 m. As shown in Figure 5, the accretion rates along the shoreline in the study area are gradual but relatively low, as indicated above the red line.

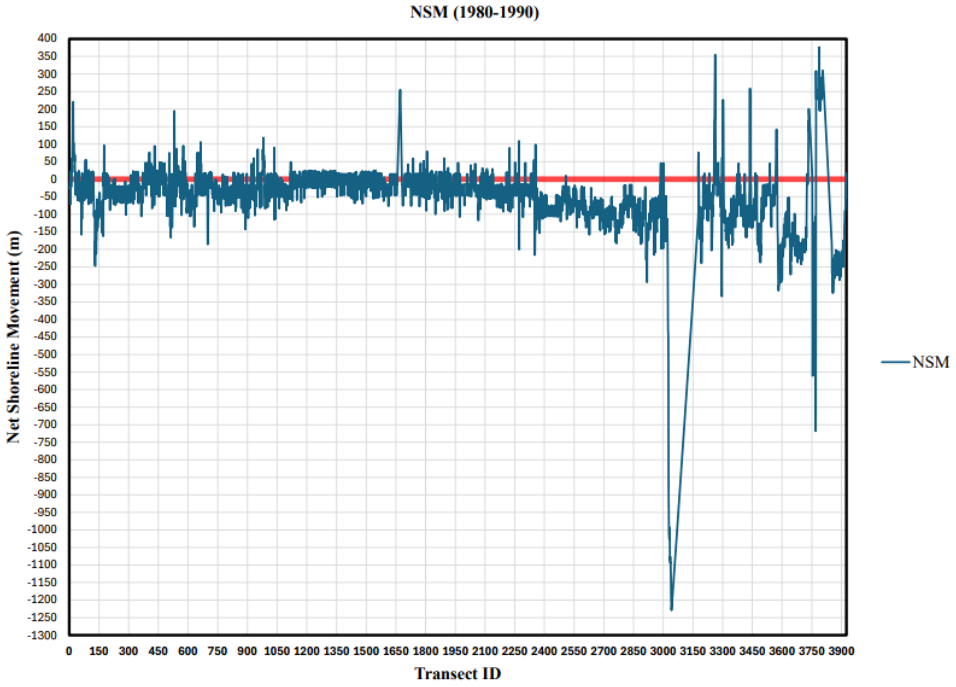

Figure 5. Illustrates the NSM results for the study area covering the period between 1980 and 1990

Figure 6 presents the SCE values and illustrates a clear spatial gradient in the distance between the 1980 and 1990 shorelines, extending from the coast of Wadi Sarr near Al Muwaylih village to Qiyal village, where the maximum distance reaches around 1229 m. Beyond this point, the distance gradually decreases from Wadi Sir toward the end of the study area at Wadi al Ayn, with the maximum separation in this section not exceeding approximately 300 m. Meanwhile, Figure 7 illustrates the erosion and accretion rates in meters per year between 1980 and 1990, where the highest erosion rate approximately -131 m/year occurred along the shoreline of Sharma village, and the highest accretion rate around 40 m/year was recorded along the shoreline of Qiyal village, both of which represent parts of the NEOM project area.

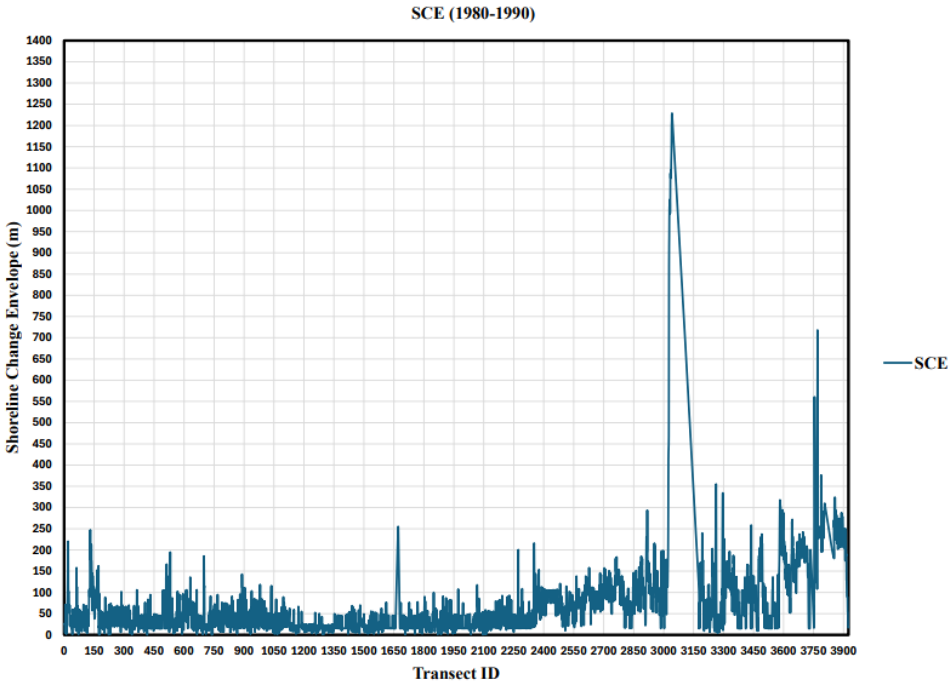

Figure 6. Illustrates the SCE results for the study area covering the period between 1980 and 1990

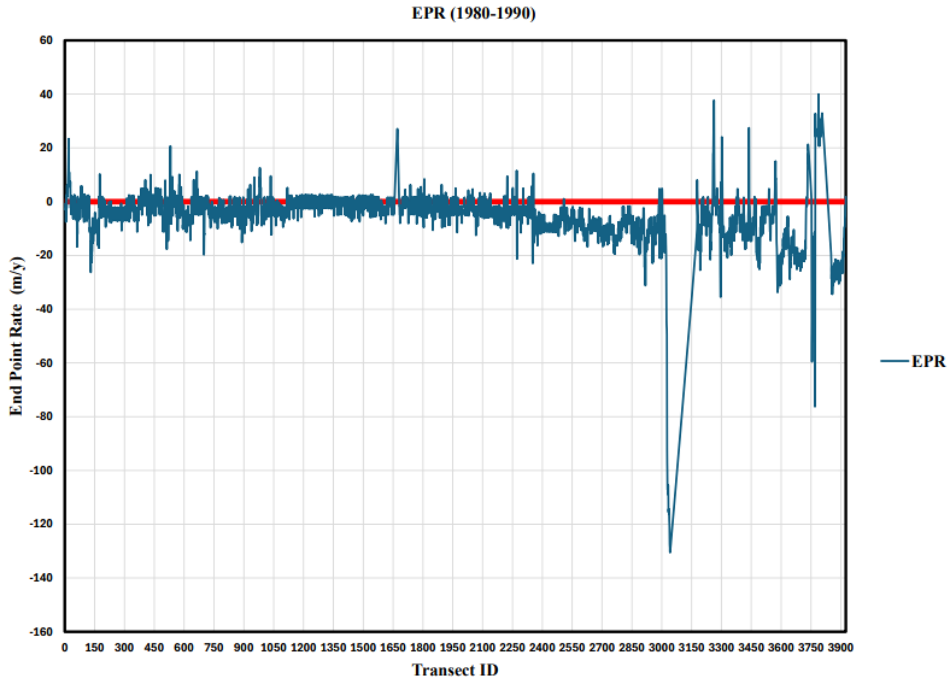

Figure 7. Illustrates the EPR results for the study area covering the period between 1980 and 1990

Figure 8 represents the NSM for the study area between 1990 and 2000. The figure shows a relatively stable shoreline during these two years, unlike the period from 1980 to 1990, where noticeable changes were observed between Sharma village shoreline and Qiyal village shoreline. This figure indicates that the highest accretion occurred between transect

3024 and transect 3189 at Sharma village shoreline, reaching a distance of 864 m. The transects adjacent to this accretion zone experienced erosion, with the highest erosion observed at a section of Sharma village shoreline at transect 3000, reaching - 244 m. Erosion was also noted from the Port of NEOM shoreline (formerly Duba Port) to Wadi al Ayn, between transect 1 and transect 664, with erosion rates ranging from -10 to -182 m. Observing the red line in the figure, it is clear that the overall erosion along the shoreline is much higher than accretion.

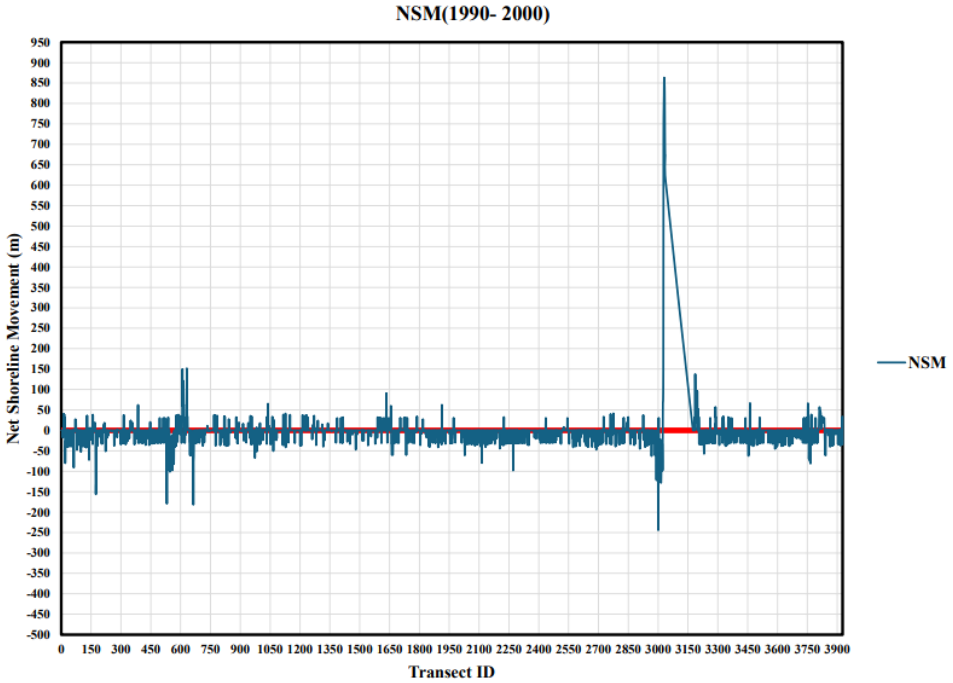

Figure 8. Illustrates the NSM results for the study area covering the period between 1990 and 2000

Figure 9 represents the SCE in meters between 1990 and 2000, showing that the maximum distance between the shorelines occurs at Sharma village, reaching approximately 864 meters. In the rest of the study area, the shoreline distances remain relatively stable, showing no significant variations, where the greatest difference does not exceed about 250 meters, while Figure 10 shows the annual rate of change (EPR) in m/year during the same period. The highest erosion rate was approximately -25 m/year at a section of Sharma village shoreline toward Qiyal village, while the highest accretion rate was about 86 m/year at a section of Sharma village shoreline toward Al Muwaylih village.

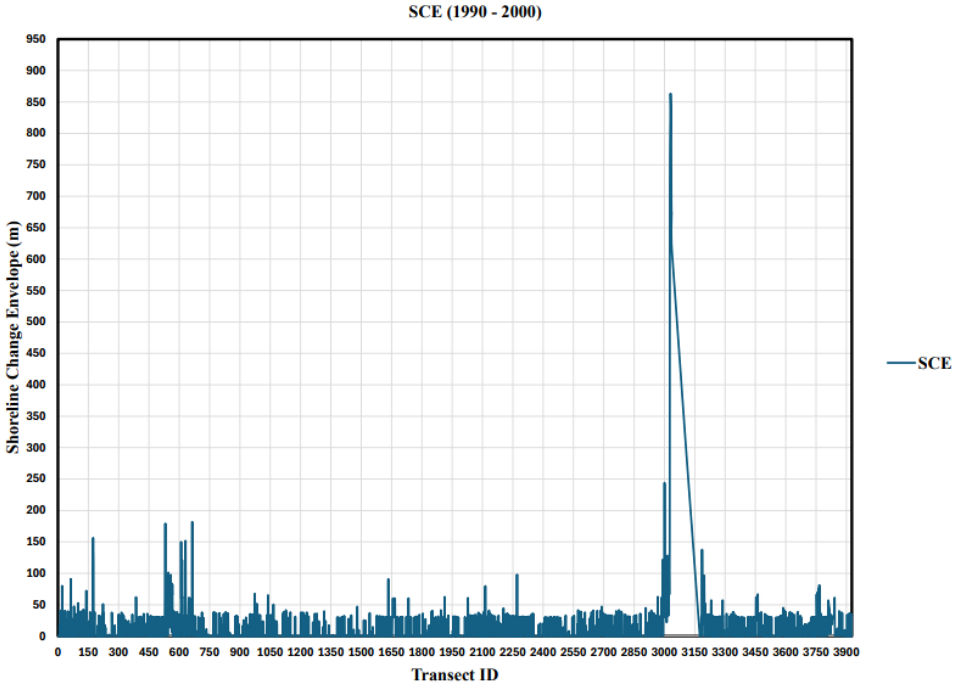

Figure 9. Illustrates the SCE results for the study area covering the period between 1990 and 2000

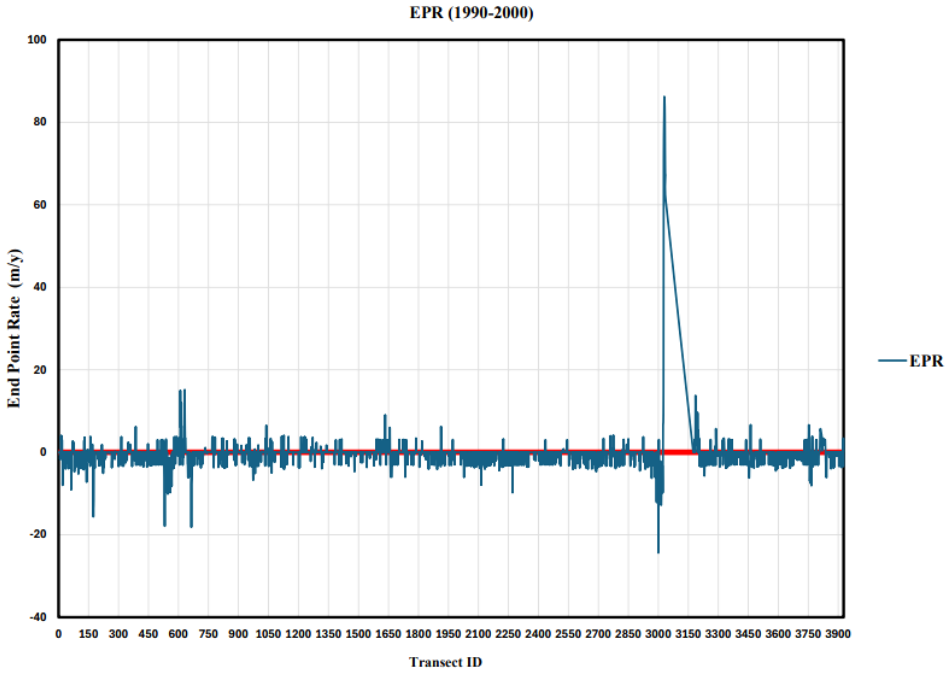

Figure 10. Illustrates the EPR results for the study area covering the period between 1990 and 2000

Figure 11 represents the NSM, which illustrates shoreline changes in terms of erosion and accretion during the period from 2000 to 2013, over 13 years. Near Wadi Sadr at As Sawrah village, between transects 2994 and 3040, the highest erosion rates were observed, with a maximum erosion of approximately - 926 m. Significant erosion was also noted at the end of Sharma village shoreline, extending past Al Khuraybah Village to Qiyal village shoreline, between transects 3186 and 3843, where maximum erosion reached around - 560 m. These villages are part of the NEOM project. From transect 1 to transect 703, along the shoreline opposite Wadi Ain and Wadi Damah, the maximum erosion reached approximately - 244 m. As shown in Figure 11, accretion along the study area's shoreline is gradual but limited, with a maximum accretion of around 270 m, indicated above the red line.

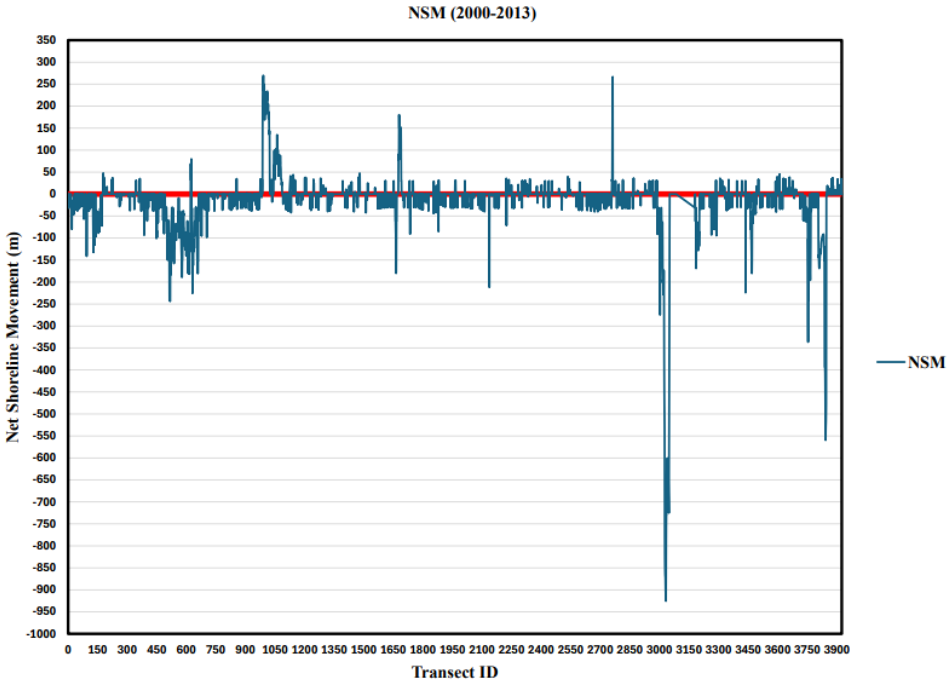

Figure 11. Illustrates the NSM results for the study area covering the period between 2000 and 2013

Figure 12 represents the SCE in meters for the period from 2000 to 2013. The figure shows that shoreline changes are irregular and exhibit noticeable disturbances. The maximum change, about 926 meters, occurred at Wadi Sadr, followed by a secondary maximum of approximately 560 meters in the direction from Wadi Sadr toward Qiyal village.

Across the rest of the study area, from Wadi Sadr to Wadi al Ayn, the maximum variation between shorelines did not exceed around 270 meters. Figure 13 illustrates the annual rate of shoreline change in meters per year during the same period. The highest erosion rate was about - 71 m/year at Sharma village shoreline, while the maximum accretion rate reached approximately 21 m/year near the shoreline of NEOM Port (formerly Duba Port).

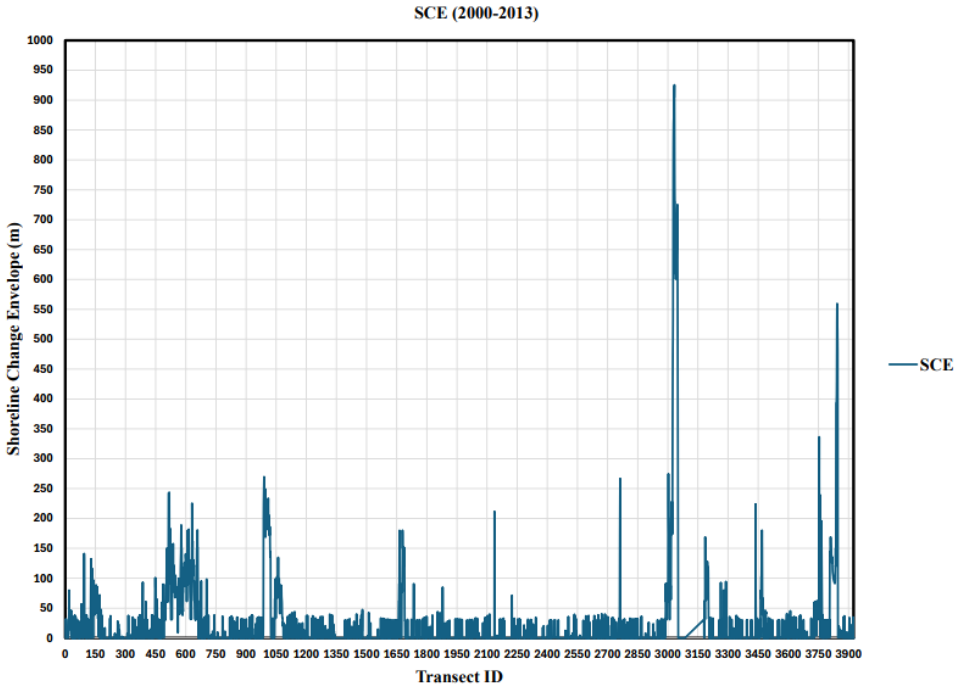

Figure 12. Illustrates the SCE results for the study area covering the period between 2000 and 2013

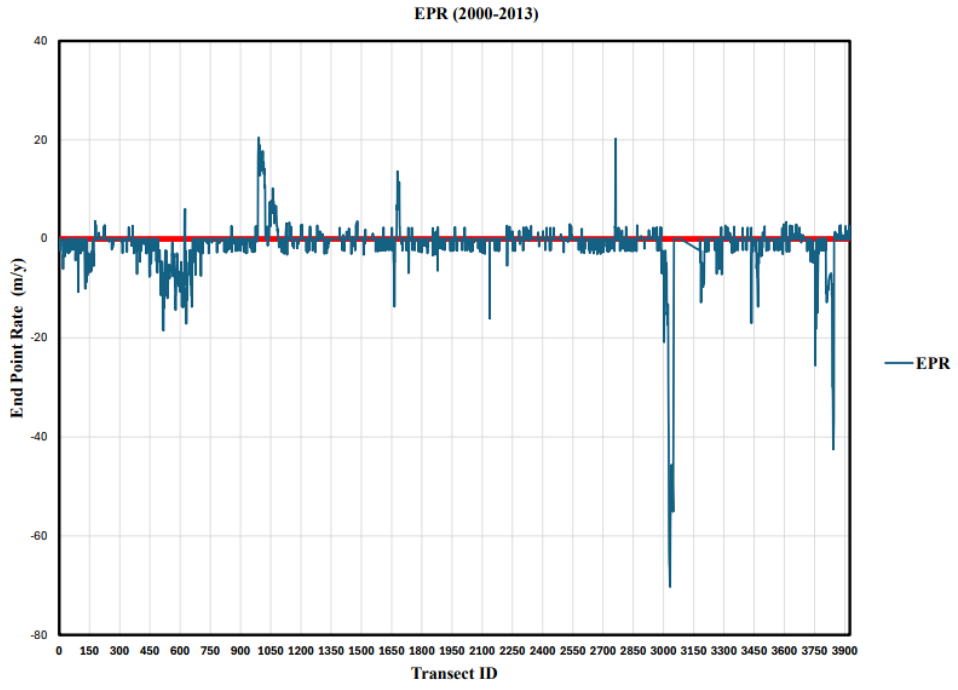

Figure 13. Illustrates the EPR results for the study area covering the period between 2000 and 2013

Figure 14 illustrates the NSM analysis of shoreline variations between 2013 and 2025. The figure shows that erosion areas along the shoreline within the study area are significantly larger than the accretion areas. This is clearly indicated by the red line in the figure, where the upper part represents accretion zones, while the lower part represents erosion zones. The highest erosion was recorded along the shoreline of NEOM Port (formerly Duba Port), where the maximum erosion reached about - 902 m between transects 1652 and 1688. The highest accretion occurred along the shoreline of Sharma village, reaching approximately 607 m between transects 3022 and 3042.

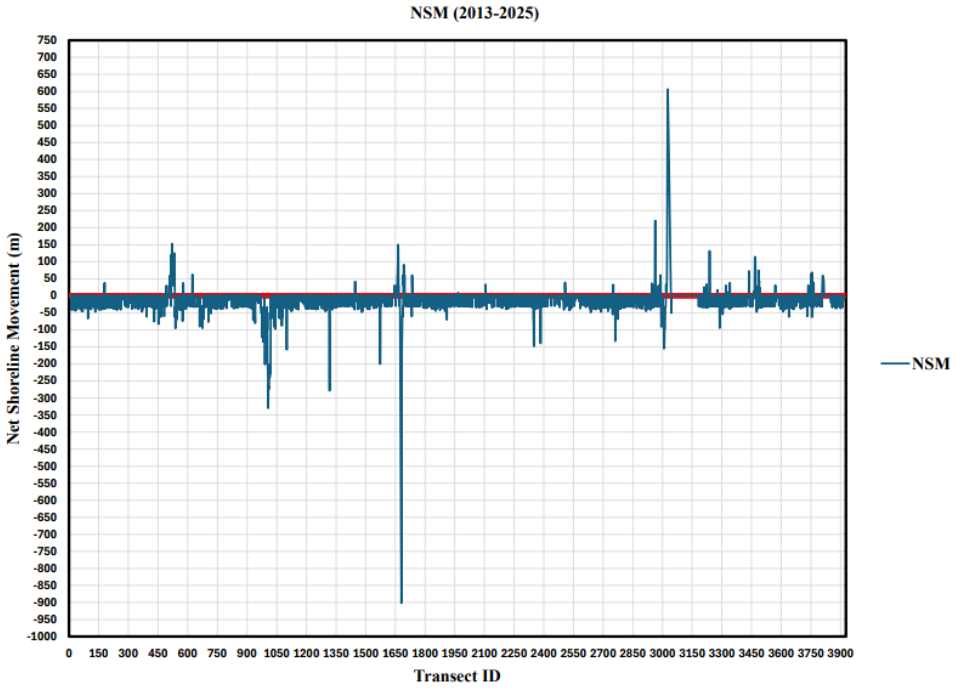

Figure 14. Illustrates the NSM results for the study area covering the period between 2013 and 2025

Additionally, the second highest erosion was also observed along the shoreline of NEOM Port (formerly Duba Port), with a value of about - 330 m between transects 941 and 1080, while the second largest accretion distance was recorded at transect 2963 in Sharma village, reaching around 221 m. Figure 15 presents the SCE, showing the distance in meters between the 2013 and 2025 shorelines. The figure reveals that shoreline change lacks a consistent spatial pattern and varies noticeably along the coast within the study area. The greatest separation, approximately 902 m, occurs along the NEOM Port shoreline, followed by a secondary maximum of about 607 m near Sharma village. Across the remaining parts of the study area, shoreline changes are more gradual, with the maximum difference not exceeding around 330 meters. Figure 16 presents the EPR, which illustrates the rate of erosion and accretion (m/year) during the same period, where the highest erosion rate was about -74 m/year along the shoreline of NEOM Port (formerly Duba Port), and the highest accretion rate was approximately 50 m/year along the shoreline of Sharma village

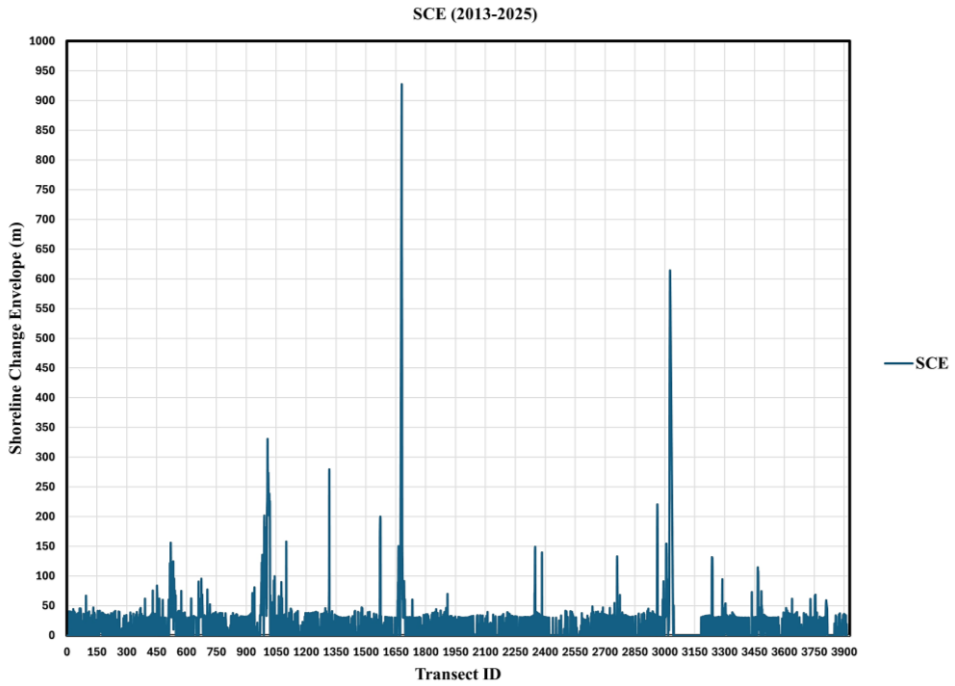

Figure 15. Illustrates the SCE results for the study area covering the period between 2013 and 2025

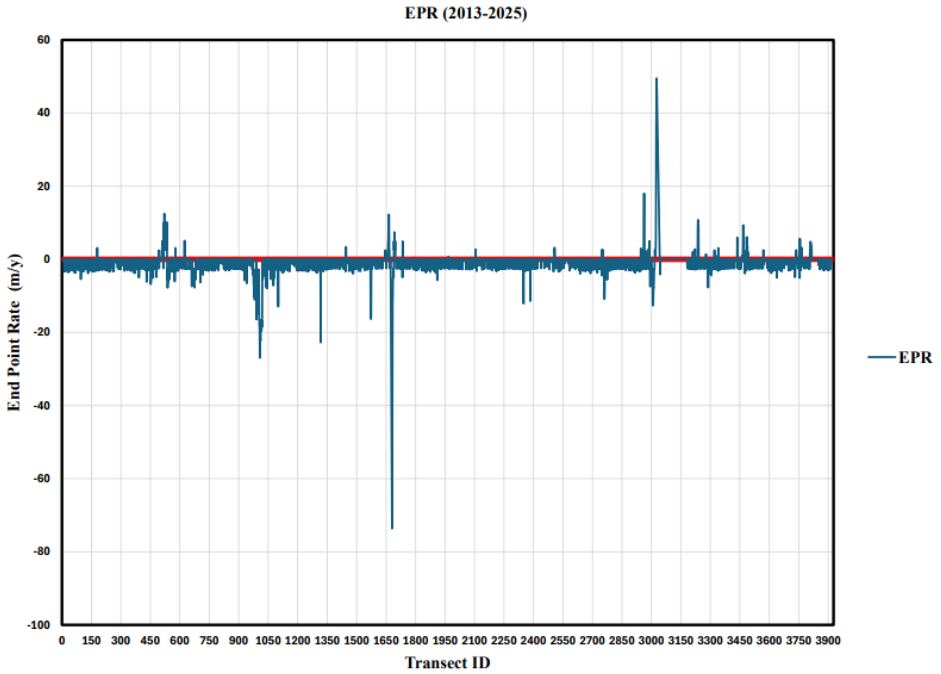

Figure 16. Illustrates the EPR results for the study area covering the period between 2013 and 2025

Figure 17 illustrates the results of the NSM, representing the distance in (meters) between shoreline positions during the period from 1980 to 2025, which indicates the areas of erosion and accretion along the study area. The figure reveals noticeable variations across several coastal segments, with the most significant erosion observed around transect 2347, located in the middle of Wadi Sarr shoreline opposite to the Jibal and Dubbagh. This area extends from Al Muwaylih village, passing through As Sawrah, Sharma, and Al Khuraybah villages, and reaching Qiyal village at the end of the transects at 3914. This section of the study area is part of the NEOM Project, and the maximum recorded erosion in this part reached approximately - 735 m. The results also show remarkable changes along the shoreline opposite NEOM Port (formerly Duba Port), covering the transects from 1133 to transect 1, which corresponds to Wadi al Ayn. However, the degree of disturbance there is lower compared to the previously mentioned area. In addition, significant erosion was recorded at Jabal Shar, reaching around - 737 m, while the shoreline stretching from NEOM Port (formerly Duba Port) to Al Muwaylih village exhibits milder erosion patterns. As shown in Figure 17, the accretion zones extending from Sharma village to Qiyal village exhibit noticeable instability and lack a consistent spatial pattern, although the overall volume of accretion remains relatively limited. The maximum recorded accretion reached approximately 355 m, while the accretion rates along the remainder of the study area are generally low and variable, with the highest rate measuring around 185 m.

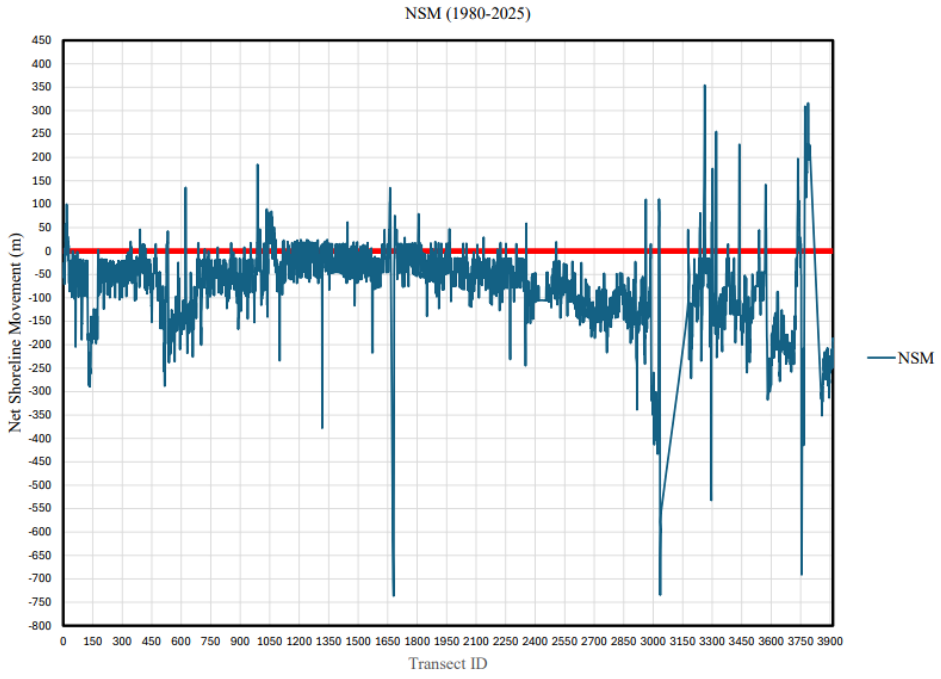

Figure 17. Illustrates the NSM results for the study area covering the period between 1980 and 2025

Meanwhile, Figure 18 presents the SCE values, representing the distance between the 1980 and 2025 shorelines within the study area. The figure indicates that shoreline changes are irregular and pronounced along the segment extending from the middle of the Wadi Sarr coast to Qiyal village, where the maximum shoreline separation reached 1848 meters. In the segment stretching from NEOM Port to Wadi al Ayn, changes were observed but remained limited, with the maximum distance between shorelines measuring 330 meters. The area between these two segments showed relative stability, whereas the transect at Jabal Shar experienced significant and pronounced changes, with the distance between shorelines reaching 2311 meters. Figure 19 also shows the EPR in meters per year during the same period, where the highest erosion rate was about -16.5 m/year along Sharma village shoreline and the area opposite Jabal Shar, while the highest accretion rate was 7.9 m/year, was also recorded near Sharma shoreline. Figure 20 shows the LRR in meters per year during the same period, where the highest erosion rate was about - 20.92 m/year, while the highest accretion rate was 5.84 m/year.

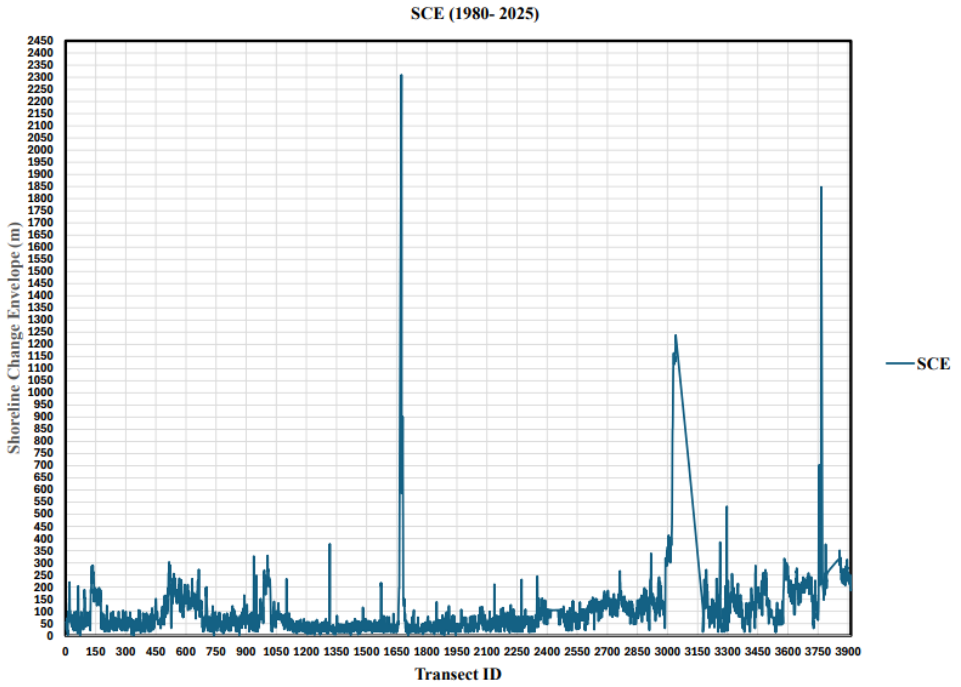

Figure 18. Illustrates the SCE results for the study area covering the period between 1980 and 2025

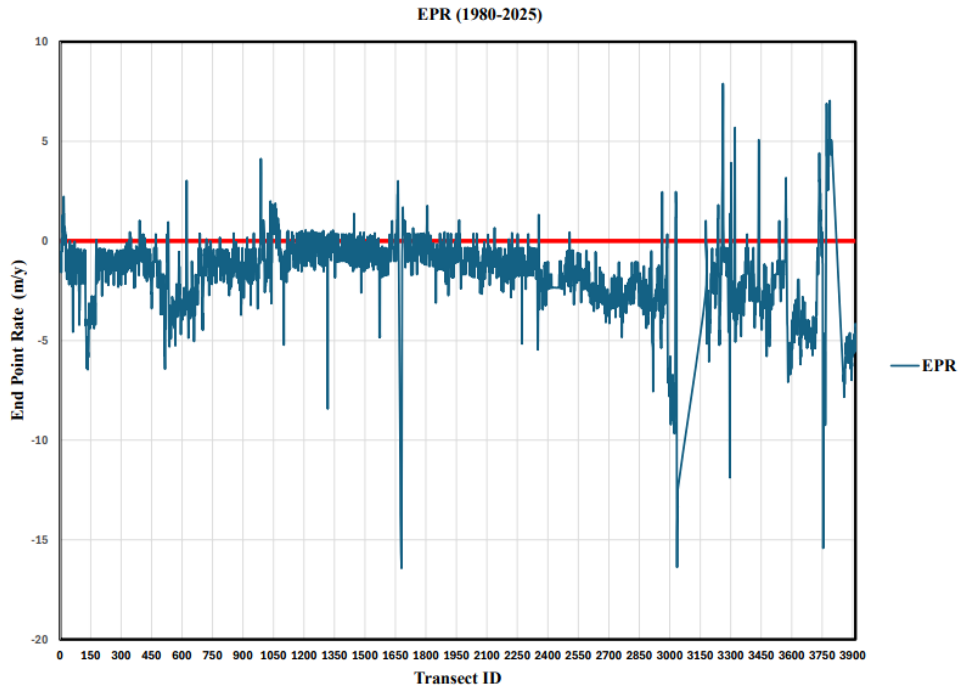

Figure 19. Illustrates the EPR results for the study area covering the period between 1980 and 2025

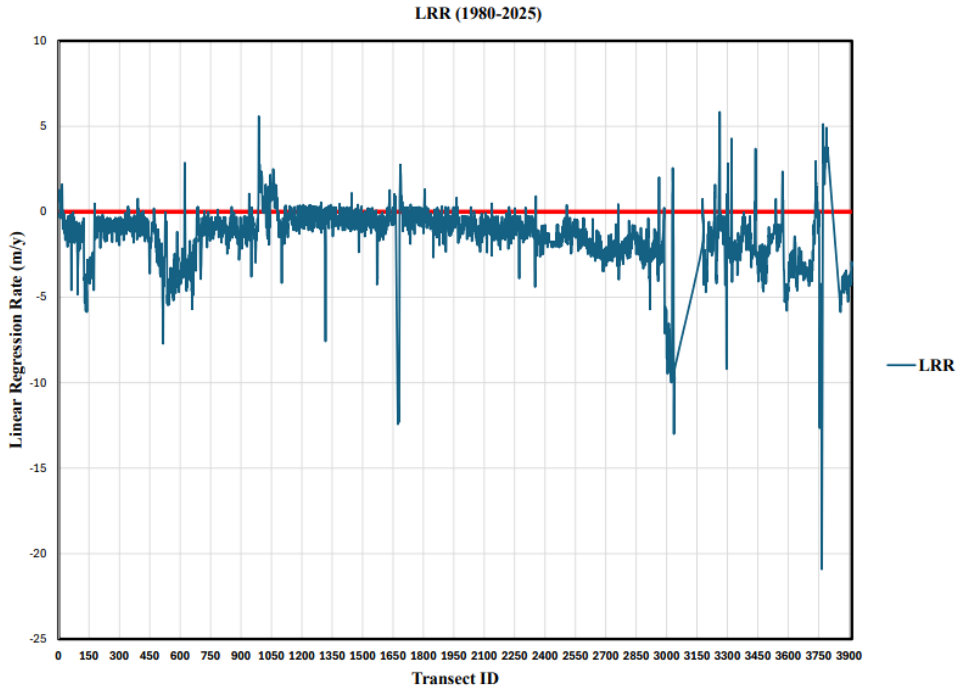

Figure 20. Illustrates the LRR results for the study area covering the period between 1980 and 2025

By analyzing the results of Figure 7, 10, 13 and 16, which illustrate the EPR for the time periods 1980–1990, 1990–2000, 2000–2013, and 2013–2025, as shown in Table 2, it is evident that the average erosion rate during the period 1980–1990 was -7.77 m/year, while the average accretion rate was 4.27 m/year. During the period 1990–2000, the average erosion rate decreased to - 2.94 m/year, whereas the average accretion rate increased to 5.42 m/year. Between 2000 and 2013, the average erosion rate rose to - 5.56 m/year, while the average accretion rate declined to 4.64 m/year. However, during the period 2013–2025, the average erosion rate decreased again to - 2.66 m/year, and the average accretion rate increased to 5.29 m/year.

Table 2. Estimated EPR values across four different time periods

Period	Erosion (m/year)			Accretion (m/year)		
	Maximum	Average	Minimum	Maximum	Average	Minimum
1980-1990	- 130.54	- 7.77	- 0.01	39.99	4.27	0.06
1990-2000	- 24.37	- 2.94	- 0.01	86.24	5.42	0.01
2000-2013	- 70.32	- 5.56	- 0.01	20.05	4.64	0.02
2013-2025	- 73.66	- 2.66	- 0.01	49.53	5.29	0.23

Table 3 summarizes the results of the NSM and SCE indicators for the different time periods, showing the maximum, minimum, and average values for each period. The results indicate that both indicators do not follow a consistent pattern, as the highest average values were recorded during the period 1980–1990, followed by a decrease in 1990–2000, an increase again in 2000–2013, and then a decline during 2013–2025. For the entire period from 1980 to 2025, the average NSM was approximately -76.72 meters, while the average SCE was around 98.19 meters.

Table 3. Presents the estimated NSM and SCE values for four different time periods

Period	NSM (m)			SCE (m)		
	Maximum	Average	Minimum	Maximum	Average	Minimum
1980-1990	376.42	-53.84	-1228.91	1228.91	67.55	0.06
1990-2000	863.38	-3.06	-243.98	863.38	12	0
2000-2013	269.76	-13.95	-925.49	925.49	23	0
2013-2025	606.46	-12.45	-901.87	901.87	17.40	0
1980-2025	354.25	-76.72	-736.53	2310.26	98.19	0.06

Figures 21 to 24 illustrate the areas of erosion and accretion along the shoreline during the time periods 1980–1990, 1990–2000, 2000–2013, and 2013–2025, respectively.

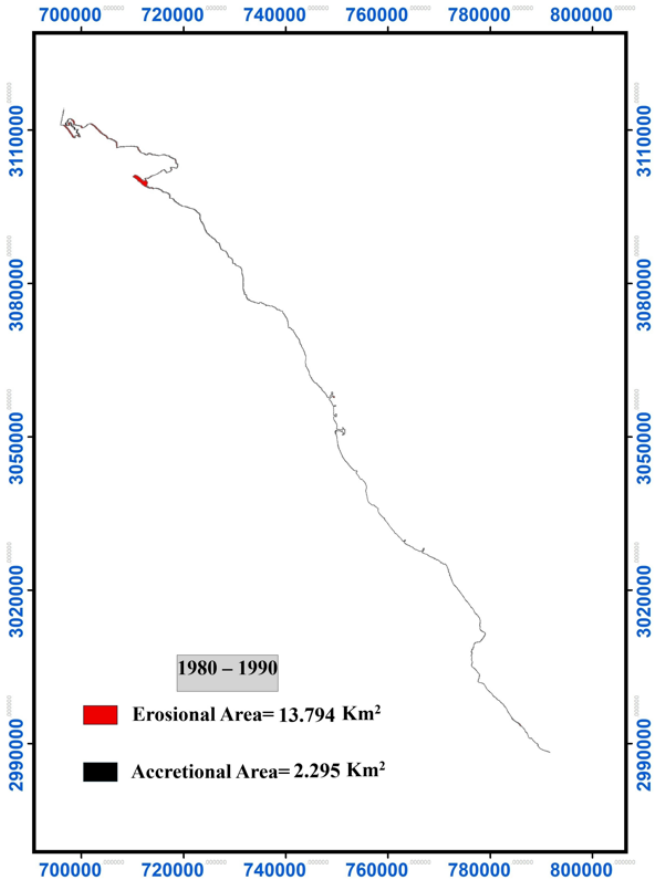

Figure 21. Shows the calculated erosion and accretion areas along the shoreline of the study area for the period from 1980 to 1990

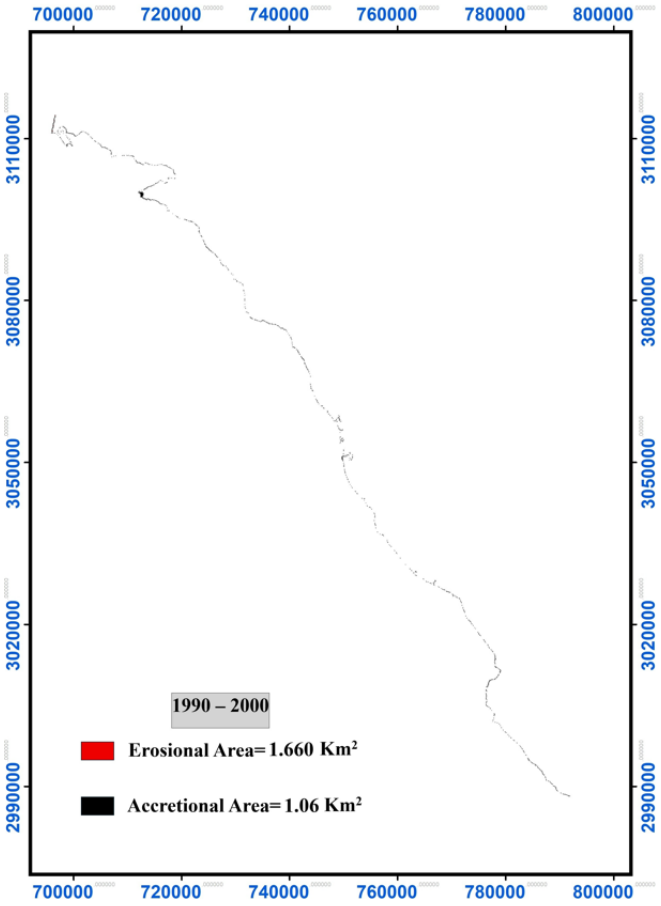

Figure 22. Shows the calculated erosion and accretion areas along the shoreline of the study area for the period from 1990 to 2000

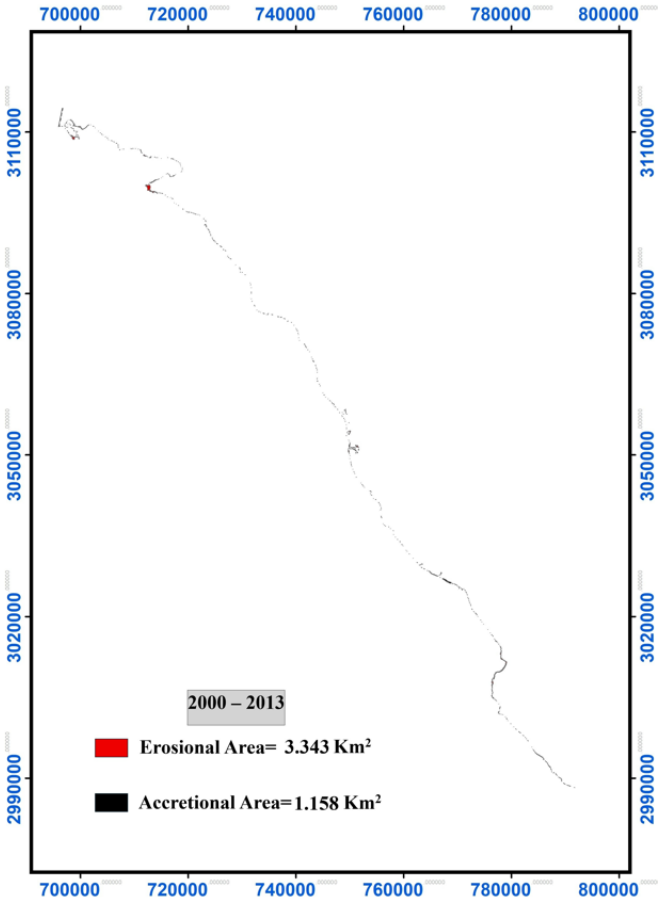

Figure 23. Shows the calculated erosion and accretion areas along the shoreline of the study area for the period from 2000 to 2013

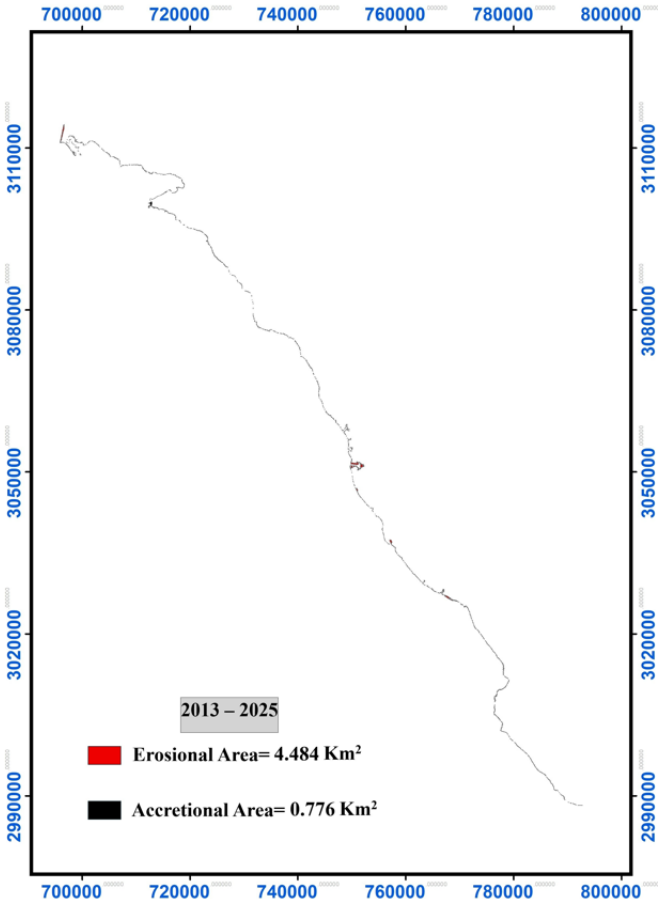

Figure 24. Shows the calculated erosion and accretion areas along the shoreline of the study area for the period from 2013 to 2025

Table 4 shows that the average erosion rate based on the EPR indicator along the shoreline during the period from 1980 to 2025 was -1.99 m/year, while the average erosion rate based on the LRR indicator was approximately -1.68 m/year. Regarding accretion rates over the same period, the average rate according to the EPR indicator was about 1.13 m/year, whereas the LRR indicator recorded an average accretion rate of 1.00 m/year. Figure 25 illustrates the erosion and accretion areas along the shoreline of the study area during the period from 1980 to 2025. Based on these results, it is evident that erosion rates were higher than accretion rates throughout this time period.

Table 4. Statistical results of EPR and NSM for the period 1980–2025

Period	Erosion (m/year)			Accretion (m/year)		
	Maximum	Average	Minimum	Maximum	Average	Minimum
EPR 1980-2025	-16.43	-1.99	-0.01	7.9	1.13	0.01
LRR 1980-2025	-20.92	-1.68	-0.02	5.84	1	0.01

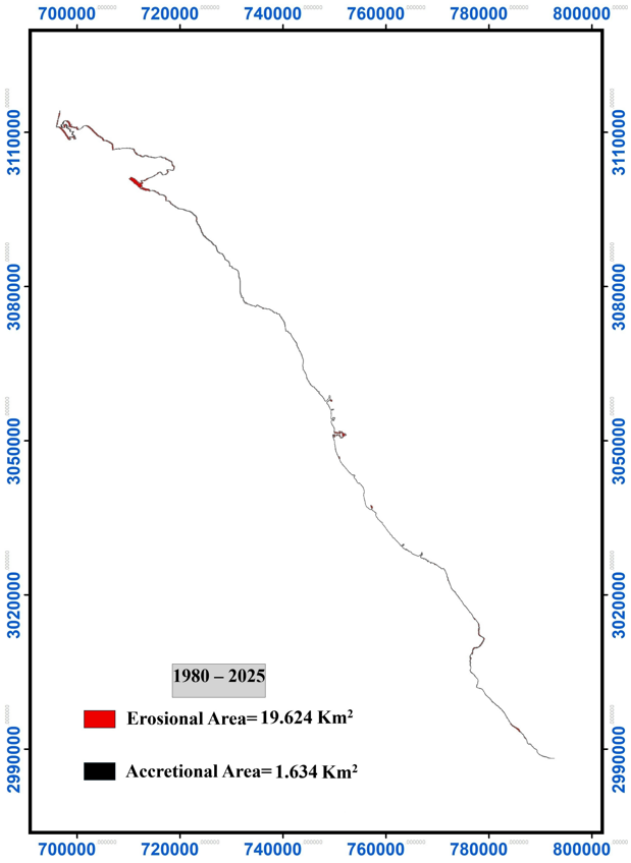

Figure 25. Computation of erosion and accretion areas along the shoreline of the study area for the period 1980–2025

Table 5 presents a collection of studies that have examined coastal changes along the Red Sea shoreline, both on the Saudi Arabian coast as previously mentioned in the introduction and on the opposite Egyptian coast, with the aim of analyzing the patterns and behavior of coastal change. The results of these studies indicate that the Red Sea coasts do not follow a consistent pattern in terms of erosion or accretion processes. Certain time periods are dominated by erosion, while others are characterized by accretion. This variation is attributed to a combination of natural and human factors, most notably human activities related to port development, the establishment of economic cities, and the expansion of infrastructure, in addition to the social and economic growth occurring in coastal regions. Furthermore, the construction of tourist resorts driven by the Red Sea's high tourism potential also influences shoreline dynamics. Climate change, sea-level rise, tidal variations, coastal waste disposal, and other human activities likewise contribute to altering the dynamics and stability of the Red Sea shorelines.

The results of the study conducted by Alamery et al. (2025) [18] along an approximately 130 km segment of the Duba coast, Saudi Arabia, indicate that the projected mean (NSM) by 2100 shows coastal erosion ranging from −8.1 m under the low-emission scenario SSP1-2.6 to −25.6 m under the high-emission scenario SSP5-8.5, with 95% confidence intervals extending to -47.9 m.

In our study area, which includes Duba Port, the results also demonstrate significant coastal erosion across all analyzed time periods. The mean NSM values range between −3.06 m and −76.72 m, confirming that the study area is experiencing continuous shoreline retreat with variable intensity from one period to another, depending on changes in the natural and anthropogenic factors controlling coastal dynamics.

Table 5. Presents an overview of the results from studies carried out on the Red Sea shorelines

Ref.	Location	Data/ Time period	Erosion Rate	Accretion Rate	Detailed Findings
Alharbi (2020) [8]	The coastline of Rabigh, Saudi Arabia	• SPOT-CIB (1986) • Landsat TM (1998) • Landsat ETM+ (2005) • Sentinel-2 (2019) • Use GIS with DSAS tool **1986 to 2019**	Changes in the Shoreline (1986–1998) The highest accretion rate was 14.68 ± 2.96 m/yr throughout this time, and the largest erosion rate was –19.76 ± 2.96 m/yr. Changes in the Shoreline (1998–2005) The greatest rates of erosion and accretion along the shoreline were –45.89 ± 5.37 m/yr and 39.35 ± 5.37 m/yr, respectively. Shoreline Changes (2005–2019) The highest recorded erosion rate was –47.21 ± 1.41 m/yr, with areas showing erosion of approximately 46 ± 1.41 m/yr.		The most significant alterations to the coastline's structure were brought about by human activity, including the growth of ports, the establishment of industrial zones, and the extension of infrastructure.
Alharbi et al. (2023) [7]	Along the Ash Shu'aybah–Al Mujayrimah coastline, Saudi Arabia	• Eight Landsat satellite images • four Sentinel-2 satellite images • Use GIS with DSAS tool **1986 to 2022**	Maximum erosion for Sentinel-2 and Landsat is - 12.02 m/yr −14.59 m/yr respectively.	Maximum accretion for Sentinel-2 and Landsat is 2.53 m/yr and 6.22 m/yr respectively.	The purpose of this study was to evaluate the pace of shoreline change and forecast the Ash Shu'aybah and Al Mujayrimah coastlines' future locations in Saudi Arabia's eastern Red Sea over a twenty-year period (2022–2042). The region is predominantly affected by erosion, with the central section experiencing particularly high erosion rates.
Al-Zubieri et al. (2018) [9]	The coastal zone of Jazan City, Saudi Arabia	• Four satellite images (TM and ETM) • ERDAS IMAGINE 2014 • ArcGIS 10.3 **1987 to 2017**	Time period (1987–2000) During this period, the landfilling and deposition area was 2.88 km², while the erosion area was 0.91 km².Time period (2000–2013) During this period, the landfilling and deposition area was 8.54 km², while the erosion area was 0.49 km². Time period (2013–2017) During this period, the landfilling and deposition area was 4.33 km², while the erosion area was 0.61 km². Time period (1987–2017) During this period, the total landfilling and deposition area was 15.76 km², while the total erosion area was 2.01 km².		The construction of a new economic metropolis in the northern section between 2003 and 2013, as well as other socioeconomic trends, are probably responsible for these changes. Landfilling has reduced the tidal flat in front of the city, which has destroyed extensive mangrove ecosystems and likely affected the local biotic communities.
Al-Zubieri et al. (2020) [10]	Shoreline between Al Lith and Ras Mahasin, Saudi Arabia	• Eight A Landsat images (TM and ETM) • ArcGIS 10.2 • ENVI software • DSAS **1984 to 2018**	The shoreline evolution rates, calculated using the LRR method, were classified into five categories: −11.84 to −7.85 m/year (very high erosion), −7.85 to −4.17 m/year (moderate erosion), −4.17 to 0.00 m/year (low erosion), 0.00 to 1.28 m/year (low accretion), and 1.28 to 14.44 m/year (high accretion). Historical shoreline positions (distance from the baseline, in meters) were determined at several sectors along the coast for the years 1984, 1986, 1990, 1994, 1998, 2014, and 2018, respectively. For the first sector, the values (in meters) were, respectively: 243.4, 236.5, 213.2, 229.6, 165, 172, 181.1.		Strong waves and longshore sediment transport largely drive shoreline variations. According to the predictive model, making much of the coast highly vulnerable to accelerated erosion.
Niang (2020) [11]	The Yanbu coastal zone, Saudi Arabia	• Multisensor and diachronic remote sensing data with high spatial resolution were utilized in this study to analyze the Yanbu coastline for the years 1965, 1980, 1988, 2000, 2010, and 2019. • ArcGIS 10.7 GIS software • ERDAS IMAGINE • DSAS **1965 to 2019**	Time period (1965–1980) During this period, the accretion area was 8.15 km², while the erosion area was 0. 10 km². Time period (1980–1988) During this period, the accretion area was 3.66 km², while the erosion area was 2.29 km². Time period (1988–2000) During this period, the accretion area was 0.18 km², while the erosion area was 0.05 km². Time period (2000–2010) During this period, the accretion area was 3.30 km², while the erosion area was 1.10 km². Time period (2010–2019) During this period, the accretion area was 3.23 km², while the erosion area was 1.00 km².		The Yanbu commercial port and other areas of the Yanbu Al Sinaiyah coast show altered patterns, according to the EPR (short-term alterations). About 20 square kilometers of water and islets have been excavated or backfilled for a variety of purposes. Therefore, human activity is linked to significant changes in the coastline's layout.
Daoudi & Niang (2021) [12]	Along the coast of Jeddah, Saudi Arabia	• Used high-spatial-resolution remote sensing data from several sources and time periods to cover the Jeddah shoreline in 1951, 1966, 1972, 1986, 2003, 2010, and 2018. • ERDAS IMAGINE software • ArcGIS software. • DSAS **1951 to 2018**	• Between 1951 and 1966, the average shoreline change was 5.72 m/yr, with a maximum accretion of 44 ± 0.52 m/yr and a minimum erosion of −7 m/yr. • From 1972 to 1986, the maximum accretion reached 180.8 ± 0.87 m/yr, while the minimum erosion was −3.4 ± 0.87 m/yr. • The lowest maximum accretion of 33.39 ± 0.67 m/yr occurred between 1986 and 2003. • Between 2003 and 2010, the average rate of erosion was 0.8 ± 0.46 m/year, the minimum rate was −0.05 ± 0.46 m/year, and the maximum rate was 107.5 ± 0.46 m/year. • From 2010 to 2018, accretion peaked at 210.93 ± 1.46 m/yr, while minimum erosion was −1.69 ± 1.46 m/yr, with an overall average of 2.27 ± 1.46 m/yr.		These changes are primarily the result of frequent land reclamation activities along this section of the coast. The rapid urban growth and economic fluctuations in Jeddah have intensified human interventions along the shoreline, including the continuous expansion of the port during the monitoring period. Approximately 23 km² of marine area and adjacent islets have been reclaimed to develop port facilities and related infrastructure.

El-Asmar et al. (2015) [41]	The coastal zone of Hurghada, Red Sea, Egypt	• The study employed multispectral satellite datasets acquired from MSS, TM, ETM+, and SPOT XS sensors for the years 1972, 1984, 1992, 2004, and 2011 to analyze temporal changes along the coastline. • ERDAS IMAGINE 10 software. • ENVI 5.0 software • ArcMap softwar **1972 to 2011**	Time period (1972–1984) During this period, the accretion area was 0.49 km², while the erosion area was 0. 35 km². Time period (1984–1992) During this period, the accretion area was 2.68 km², while the erosion area was 0.37 km². Time period (1992–2004) During this period, the accretion area was 3.32 km², while the erosion area was 0.44 km². Time period (2004–2011) During this period, the accretion area was 1.07 km², while the erosion area was 1.51 km². Time period (1972–2011) During this period, the accretion area was 5.65 km², while the erosion area was 0.64 km².		This study shows how the shoreline has changed as a result of dredging and landfilling along the coast for resort facilities, which has led to an increase in urban area. In order to maintain a 200-meter set-back zone and expand the beach, resort construction involves dredging and landfilling on the reef flat.
Nassar et al. (2021) [42]	Along the coast of Hurghada, Red Sea, Egypt	• Multi-temporary images; high resolution Worldview, Landsat 5, 7, 8, MMS; and sentinel. • ArcGIS 10.5 software • DSAS 4.3 **1987 to 2019**	Coastline changes along Hurghada and ElGouna coast. 1987- 2019 -7.73 m/yr 2011- 2014 -20.52 m/yr 1987- 1995 -29.54 m/yr 1995- 2003 -23.48 m/yr 2003-2010 -75.77 m/yr 2010- 2016 -59.87 m/yr 2016- 2019 -149.57 m/yr 2019- 2050 -16.52 m/yr	Coastline changes along Hurghada and ElGouna coast. 1987- 2019 +24.01 m/yr 2011- 2014 +24.53 m/yr 1987- 1995 +66.8 m/yr 1995- 2003 +78.86 m/yr 2003-2010 +77.44 m/yr 2010- 2016 +31.95 m/yr 2016- 2019 +203.9 m/yr 2019- 2050 +9.21 m/yr	From an ecological and financial perspective, the coastal regions around Hurghada at risk of erosion and accretion. The majority of this issue has been brought on by human activity and beach waste disposal.
Dewidar (2011) [43]	The shoreline between Marsa Alam and Hamata, Red Sea, Egypt	• Landsat MSS • Landsat TM • Landsat ETM+ • Tera ASTER • ERDAS Imagine software • DSAS version 3.2 **1971 - 2007**	Shoreline erosion and accretion rates in the study area exhibited temporal changes between 1972–1990 and 1990–2007. Alongshore trends shifted from accretion to erosion near Abu Datab (5.5 to –2.5 m/yr), while Marsa Um Tondoba experienced dominant erosion (–3.7 to –1.2 m/yr). Five kilometers west of Ras Hon Korab, the trend reversed from erosion to accretion at 1.5 m/yr.		This study indicates that remote sensing can effectively support long-term monitoring of coastline erosion and accretion when field data are unavailable. Observed changes in alongshore rates suggest that erosion and accretion patterns are influenced by coastal processes and climate change.
Alamery et al. (2025) [18]	Along the Coast of Duba, Saudi Arabia	Analysis of Landsat satellite imagery using a sequential series of numerical models. **1985–2024**	The projected mean (NSM) by 2100 is estimated to range from −8.1 m under the low-emission SSP1-2.6 scenario to a critical −25.6 m under the high-emission SSP5-8.5 scenario, with 95% confidence intervals extending to −47.9 m.		This erosion is primarily driven by a projected relative sea-level rise of up to 48.3 cm (±15.8 cm), accompanied by an increase in significant wave height of up to 40%, with a mean value of 1.95 m.

5. Conclusion and Recommendations

Through the analysis of the study area extending between Qiyal Village and Wadi al Ayn over a period of 45 years, based on Landsat satellite imagery, Geographic Information System (GIS) techniques, and the Digital Shoreline Analysis System (DSAS) tool, the following findings were obtained:

- During the period from 1980 to 2025, the results indicated that the study area, which includes the villages of Al Muwaylih, As Sawrah, Sharma, Al Khuraybah, and Qiyal, representing part of the NEOM project along the Red Sea coast has experienced high rates of shoreline erosion. It was observed that this erosion does not follow a consistent pattern but rather exhibits fluctuation and instability. Although accretion rates were also recorded in this section, they remain significantly lower compared to the prevailing erosion rates along this part of the coast.
- During the period from 1980 to 2025, the results showed that the section of the study area extending from NEOM Port (formerly Duba Port) to Wadi al Ayn experienced shoreline erosion, though its intensity was lower than the erosion recorded in the NEOM project area, while accretion processes were very limited in this part. In contrast, the section extending from Al Muwaylih village to the Jabal Shar shoreline, located before NEOM Port, exhibited both erosion and accretion, with erosion being more dominant, reaching its maximum values in front of Jabal Shar.
- During the period from 1980 to 1990, erosion was severe and pronounced along the shoreline, with significant changes and disturbances particularly observed in the areas surrounding the villages within the NEOM project.
- During the period from 1990 to 2000, the erosion area along the shoreline in the study area was larger than the accretion area. However, both erosion and accretion processes during this stage exhibited relative stability along the coast.
- During the period from 2000 to 2013, the erosion area along the shoreline was larger than the accretion area, with notable disturbances in erosion, particularly in the areas surrounding the villages of the NEOM project, as well as in the section extending from NEOM Port to Wadi al Ayn.
- During the period from 2013 to 2025, it was observed that the erosion area along the shoreline greatly exceeded the accretion area, with no significant disturbances in either erosion or accretion along the coast.
- The analysis results indicate that the pattern of erosion and accretion in the study area does not follow a consistent trend across the different time periods, which aligns with previous studies on the Red Sea coasts. The erosion area during the period 1980–1990 reached about 13.794 km², then decreased significantly to 1.660 km² during 1990–2000. In the period from 2000–2013, the erosion area increased again to 3.343 km² and continued to rise, reaching 4.484 km² during 2013–2025. As for the accretion area, it was about 2.295 km² during 1980–1990, then decreased to 1.06 km² during 1990–2000, increasing slightly to 1.158 km² during 2000–2013, and then declining again to 0.776 km² during 2013–2025. Considering the entire period from 1980 to 2025, the total erosion area amounted to about 19.624 km², while the total accretion area reached about 1.634 km².
- The analysis results of shoreline spatial changes during the four time periods (1980–1990), (1990–2000), (2000–2013), and (2013–2025) revealed a clear variation in the rates of erosion and accretion between each period. The findings indicate that the study area, which includes the five villages (Al Muwaylih, As Sawrah, Sharma, Al Khuraybah, and Qiyal), forming part of the NEOM project zone, in addition to the area extending from NEOM Port to Wadi al Ayn, is among the regions most affected by erosion throughout the different study periods, particularly between 1980 and 2025. The highest recorded erosion rate reached about -16.43 m/year, while the maximum accretion rate was 7.9 m/year along the shoreline during the 45-year study period. These results highlight the importance of continuous monitoring and observation of coastal changes in the region using high-resolution satellite imagery supported by ground data, with the goal of improving measurement accuracy and assessing future coastal risks especially in light of the significant urban and tourism expansion taking place within the NEOM project, one of the strategic initiatives under Saudi Vision 2030. The study area also includes NEOM Port (formerly Duba Port), considered one of the world's most advanced, efficient, and sustainable ports due to its strategic location on the Red Sea coast in northwestern Saudi Arabia and its vital role in supporting economic growth in the NEOM project and surrounding areas. Additionally, the region contains NEOM Bay Airport, which serves as a key facility supporting development and construction activities within the project.

6. Declarations

6.1. Data Availability Statement

The data presented in this study are available in the article.

6.2. Funding and Acknowledgments

The author extends his appreciation to Prince Sattam bin Abdulaziz University for funding this research work through the project number (PSAU/2025/01/32386).

6.3. Conflicts of Interest

The author declares no conflict of interest.

7. References

[1] Darwish, K. S. (2024). Monitoring Coastline Dynamics Using Satellite Remote Sensing and Geographic Information Systems: A Review of Global Trends. Catrina: The International Journal of Environmental Sciences, 31.1 (2024), 1–23. doi:10.21608/cat.2024.233931.1196.

[2] Ramachandran, A., Sujatha, M., Alruwais, N., & Alshahrani, H. M. (2025). Forecasting coastal stability: Digital shoreline analysis system and machine learning techniques in evaluating Impacts of cyclones. Regional Studies in Marine Science, 81, 103961. doi:10.1016/j.rsma.2024.103961.

[3] Gopinath, G., Thodi, M. F. C., Surendran, U. P., Prem, P., Parambil, J. N., Alataway, A., Al-Othman, A. A., Dewidar, A. Z., & Mattar, M. A. (2023). Long-Term Shoreline and Islands Change Detection with Digital Shoreline Analysis Using RS Data and GIS. Water (Switzerland), 15(2), 244. doi:10.3390/w15020244.

[4] Dahy, B., Al-Memari, M., Al-Gergawi, A., & Burt, J. A. (2024). Remote sensing of 50 years of coastal urbanization and environmental change in the Arabian Gulf: a systematic review. Frontiers in Remote Sensing, 5(1422910). doi:10.3389/frsen.2024.1422910.

[5] Qwaider, S., Al-Ramadan, B., Shafiullah, M., Islam, A., & Worku, M. Y. (2023). GIS-Based Progress Monitoring of SDGs towards Achieving Saudi Vision 2030. Remote Sensing, 15(24), 5770. doi:10.3390/rs15245770.

[6] Isha, I. B., & Adib, M. R. M. (2020). Application of geospatial information system (GIS) using digital shoreline analysis system (DSAS) in determining shoreline changes. IOP Conference Series: Earth and Environmental Science, 616(1), 12029. doi:10.1088/1755-1315/616/1/012029.

[7] Alharbi, O. A., Hasan, S. S., Fahil, A. S., Mannaa, A., Rangel-Buitrago, N., & Alqurashi, A. F. (2023). Shoreline change rate detection applying the DSAS technique on low and medium resolution data: Case study along Ash Shu'aybah-Al Mujayrimah coastal Area of the Eastern Red Sea, Saudi Arabia. Regional Studies in Marine Science, 66, 103118. doi:10.1016/j.rsma.2023.103118.

[8] Alharbi, O. A. A. (2020). Shoreline Change Analysis Along the Rabigh Coast of Saudi Arabia, Using Multi-Temporal Satellite Imagery. Journal of King Abdulaziz University Marine Sciences, 30(2), 33–57. doi:10.4197/mar.30-2.3.

[9] Al-Zubieri, A. G., Bantan, R. A., Abdalla, R., Antoni, S., Al-Dubai, T. A., & Majeed, J. (2018). Application Of Gis and Remote Sensing to Monitor the Impact of Development Activities on the Coastal Zone of Jazan City on the Red Sea, Saudi Arabia. The International Archives of the Photogrammetry, Remote Sensing and Spatial Information Sciences, XLII-3/W4, 45–50. doi:10.5194/isprs-archives-xlii-3-w4-45-2018.

[10] Al-Zubieri, A. G., Ghandour, I. M., Bantan, R. A., & Basaham, A. S. (2020). Shoreline Evolution Between Al Lith and Ras Mahāsin on the Red Sea Coast, Saudi Arabia Using GIS and DSAS Techniques. Journal of the Indian Society of Remote Sensing, 48(10), 1455–1470. doi:10.1007/s12524-020-01169-6.

[11] Niang, A. J. (2020). Monitoring long-term shoreline changes along Yanbu, Kingdom of Saudi Arabia using remote sensing and GIS techniques. Journal of Taibah University for Science, 14(1), 762–776. doi:10.1080/16583655.2020.1773623.

[12] Daoudi, M., & Niang, A. J. (2021). Detection of shoreline changes along the coast of Jeddah and its impact on the geomorphological system using GIS techniques and remote sensing data (1951–2018). Arabian Journal of Geosciences, 14(13), 1265. doi:10.1007/s12517-021-07605-2.

[13] Alharbi, O. A., & Niang, A. J. (2025). Shoreline Development During a Four-Decade Period, Along Al Qunfudhah Coast, Saudi Arabia. Coasts, 5(4), 45. doi:10.3390/coasts5040045.

[14] Colak, A. T. I. (2024). Geospatial analysis of shoreline changes in the Oman coastal region (2000-2022) using GIS and remote sensing techniques. Frontiers in Marine Science, 11, 1305283. doi:10.3389/fmars.2024.1305283.

[15] Teillet, T., Bois, P., Homewood, P., Mettraux, M., Samimi-Namin, K., & Vahrenkamp, V. (2025). Multidecadal Morphodynamic evolution of shorelines and coral reefs along the Arabian Sea Coast of Oman: Bar Al Hikman Peninsula. Journal of Coastal Conservation, 29(1), 17. doi:10.1007/s11852-024-01087-6.

[16] Daoudi, M. b. A., Abu Zaid, M. S. A. & Al-Ajami, M. M. (2024). Coastal changes and their environmental impacts in Jeddah, Saudi Arabia. (2024). Egyptian Journal of Environmental Change, 16(5), 67–96. doi:10.21608/egjec.2024.381007 (In Arabic).

[17] Sarrau, J., Al Abdouli, K., & Abuelgasim, A. (2025). Spatiotemporal variations of the United Arab Emirates coastline each decade from 1991 to 2021. Frontiers in Remote Sensing, 6. doi:10.3389/frsen.2025.1468918.

[18] Alamery, E. R., El Melki, M. N., Faqeih, K. Y., Alamri, S. M., Alamry, J. Y., & Alasiri, F. M. M. (2025). Bayesian Projections of Shoreline Retreat Under Climate Change Along the Arid Coast of Duba, Saudi Arabia. Sustainability (Switzerland), 17(22), 10401. doi:10.3390/su172210401.

[19] PROJECT NEOM (2026). Saudi vision 2030, NEOM, Riyadh, Saudi Arabia. Available online: https://www.vision2030.gov.sa/en/explore/projects/neom (accessed on December 2025).

[20] Official Map of Kingdom of Saudi Arabia (2026). General Authority for Survey and Geospatial Information, Riyadh, Saudi Arabia. Available online: https://www.geoportal.sa/Geoportal/GeospatialOpenData/OfficialSaudiMap (accessed on December 2025). (In Arabic).

[21] Scribble Maps (2026). Scribble Maps, Windsor, Canada. Available online: https://www.scribblemaps.com/maps/view/NEOM/jqtPQ7p6Lw (accessed on December 2025).

[22] NEOM (2026). NEOM and SAUDIA offer regular international service from NEOM Bay Airport, NEOM, Riyadh, Saudi Arabia. Available online: https://www.neom.com/ar-sa/newsroom/neom-and-saudia (accessed on December 2025).

[23] SPA (2026). The Saudi Press Agency (SPA), Riyadh, Saudi Arabia. Available online: https://www.spa.gov.sa/1939885 (accessed on December 2025).

[24] NEOM (2026). A New Future: NEOM is a region in the making in northwest Saudi Arabia. NEOM, Riyadh, Saudi Arabia. Available online: https://www.neom.com/ar-sa (accessed on December 2025).

[25] Siyal, A. A., Solangi, G. S., Siyal, Z. ul A., Siyal, P., Babar, M. M., & Ansari, K. (2022). Shoreline change assessment of Indus delta using GIS-DSAS and satellite data. Regional Studies in Marine Science, 53. doi:10.1016/j.rsma.2022.102405.

[26] Earth Explorer (2026). Earth Explorer: U.S. Department of the Interior, Washington, United States. Available online: https://earthexplorer.usgs.gov (accessed on December 2025).

[27] USGS (2026). Digital Shoreline Analysis System (DSAS), U.S. Department of the Interior, Washington, United States. Available online: https://code.usgs.gov/cch/dsas (accessed on December 2025).

[28] Aziz, K. M. A. (2024). Quantitative Monitoring of Coastal Erosion and Changes Using Remote Sensing in a Mediterranean Delta. Civil Engineering Journal (Iran), 10(6), 1842–1862. doi:10.28991/CEJ-2024-010-06-08.

[29] Baig, M. R. I., Ahmad, I. A., Shahfahad, Tayyab, M., & Rahman, A. (2020). Analysis of shoreline changes in Vishakhapatnam coastal tract of Andhra Pradesh, India: an application of digital shoreline analysis system (DSAS). Annals of GIS, 26(4), 361–376. doi:10.1080/19475683.2020.1815839.

[30] Nerves, A., Rivera, F. D., Blanco, A., Tirol, Y., & Nadaoka, K. (2024). Shoreline Change Analysis in New Washington, Aklan using Digital Shoreline Analysis System (DSAS). ISPRS Annals of the Photogrammetry, Remote Sensing and Spatial Information Sciences, X-5–2024, 111–117. doi10.5194/isprs-annals-x-5-2024-111-2024.

[31] Thieler, E. R., Himmelstoss, E. A., Zichichi, J. L., & Ergul, A. (2009). The Digital Shoreline Analysis System (DSAS) Version 4.0 - An ArcGIS extension for calculating shoreline change. Open-File Report, 2008-1278. doi:10.3133/ofr20081278.

[32] Elia, A. K. (2005). Risk Evolution of the coastline in Lebanon between 1962 and 2003. Master Thesis, ESGT, Le Mans, France. (In French).

[33] Adebola, A. O., Komolafe, A. A., Adegboyega, S. A., & Ibitoye, M. O. (2017). Time series analysis of shoreline changes along the coastline of Rivers State, Nigeria. Ife Research Publications in Geography, 15, 63-77.

[34] Brooks, S. M., & Spencer, T. (2010). Temporal and spatial variations in recession rates and sediment release from soft rock cliffs, Suffolk coast, UK. Geomorphology, 124(1–2), 26–41. doi:10.1016/j.geomorph.2010.08.005.

[35] Saad, R., Gerard, J. A., & Gerard, P. (2021). Detection of the shoreline changes using DSAS technique and remote sensing: a case study of Tyre Southern Lebanon. Journal of Oceanography and Marine Research, 9(11), 1000004.

[36] Song, Y., Shen, Y., Xie, R., & Li, J. (2021). A DSAS-based study of central shoreline change in Jiangsu over 45 years. Anthropocene Coasts, 4(1), 115–138. doi:10.1139/anc-2020-0001.

[37] Zorlu, O., & Kusak, L. (2025). An assessment of the long-term change of the Mersin west coastline using digital shoreline analysis system and detection of pattern similarity using fuzzy C-means clustering. Frontiers in Marine Science, 12. doi:10.3389/fmars.2025.1457016.

[38] Christofi, D., Mettas, C., Evagorou, E., Stylianou, N., Eliades, M., Theocharidis, C., Chatzipavlis, A., Hasiotis, T., & Hadjimitsis, D. (2025). A Review of Open Remote Sensing Data with GIS, AI, and UAV Support for Shoreline Detection and Coastal Erosion Monitoring. Applied Sciences (Switzerland), 15(9), 4771. doi:10.3390/app15094771.

[39] Pradana, M. R., & Semedi, J. M. (2025). Effortless coastal monitoring: Unsupervised detection of shoreline alterations due to tin mining in Bangka Belitung. IOP Conference Series: Earth and Environmental Science, 1462(1), 12004. doi:10.1088/1755-1315/1462/1/012004.

[40] Zoysa, S., Basnayake, V., Samarasinghe, J. T., Gunathilake, M. B., Kantamaneni, K., Muttil, N., Pawar, U., & Rathnayake, U. (2023). Analysis of Multi-Temporal Shoreline Changes Due to a Harbor Using Remote Sensing Data and GIS Techniques. Sustainability (Switzerland), 15(9), 7651. doi:10.3390/su15097651.

[41] El-Asmar, H. M., Ahmed, M. H., El-Kafrawy, S. B., Oubid-Allah, A. H., Mohamed, T. A., & Khaled, M. A. (2015). Monitoring and assessing the coastal ecosystem at Hurghada, Red Sea Coast, Egypt. Journal of Environment and Earth Science, 5(6), 144–160.

[42] Nassar, K., El-Adawy, A., Zakaria, M., Diab, R., & Masria, A. (2022). Quantitative appraisal of naturalistic/anthropic shoreline shifts for hurghada: Egypt. Marine Georesources and Geotechnology, 40(5), 573–588. doi:10.1080/1064119X.2021.1918807.

[43] Dewidar, K. (2011). Changes in the Shoreline Position Caused by Natural Processes for Coastline of Marsa Alam – Hamata, Red Sea, Egypt. International Journal of Geosciences, 2(4), 523–529. doi:10.4236/ijg.2011.24055.